Explicit ARL Formulas on DEWMA Chart for Seasonal Autoregressive Model with Application in Air Pollution

Yupaporn Areepong, Kotchaporn Karoon

Abstract—**Process monitoring is frequently done with quality control charts. To find tiny and moderate shifts in the process, the DEWMA control chart is a useful choice. The purpose of this article is to construct precise formulas for the average run length (ARL) in order to improve usability with observations from a seasonal autoregressive model. The Fredholm integral equation has been used to solve the explicit formula, and Banach's fixed point theorem has been used to guarantee the solution's uniqueness. The explicit formula's accuracy was checked using the numerical integral equation, also known as the NIE approach. And then, its efficiency was proven by the computation's speed. The results of the new ARL's explicit formula were compared with the NIE in relative error (RE). It is calculated as less than 10^{-5} %. One significant finding from this comparison is that the calculation, in terms of the computation's speed, i.e., the explicit formula, occurs practically instantly. It was also extended to evaluate the effectiveness of the control chart between the original EWMA control chart and the suggested ARL's DEWMA control chart. This study covered both simulated and real-world data, and the findings showed likewise. And then, the application in this study was chosen to be about air pollution, which is one of the pollution's problems in Thailand.**

Index Terms— **average run length, control chart, explicit formula, numerical integral equation, seasonal autoregressive**

I. INTRODUCTION

A mix of statistical and analytical techniques called statistical process control (SPC) is very helpful in raising the caliber of a manufacturing process. Control charts are essential tools for the SPC principle. It is used to monitor processes and detect changes. It is also often applied in the environment, industry, health care, and other fields [1-3]. Shewhart [4] was the one who first proposed the concept of process validation using control charts. The Shewhart control chart has been included in many production procedures, and it is useful for detecting large changes in the mean of a process. Unfortunately, it is useless for detecting subtle or mild changes. As answers to this issue, Page [5] and Roberts [6] proposed the cumulative sum control chart (CUSUM) and

Y. Areepong is a Professor of Applied Statistics Department, King Mongkut's University of Technology North Bangkok, Bangkok, 10800, Thailand, (e-mail: yupaporn.a@sci.kmutnb.ac.th).

K. Karoon is a lecturer of Mathematics Department, Naresuan University, Phitsanulok, 65000, Thailand, (corresponding author to provide e-mail: kotchapornk@nu.ac.th).

the exponentially weighted moving average control chart (EWMA), respectively. They are capable of detecting small and moderate changes. Many researchers have developed EWMA control charts to increase control charts' capabilities in detecting small changes. Patel and Divecha [7] introduced the modified exponentially weighted moving average control chart (MEWMA), which was later developed by Khan et al. [8]. Naveed et al. [9] suggested the extended exponentially weighted moving average control chart (EEWMA). This performs better in detecting even subtle changes than the EWMA control chart shown by Karoon et al. [10]. In addition, Mahmoud and Woodall [11] suggested the double exponentially weighted moving average control chart (DEWMA). Shamma and Shamma [12] first showed it in 1992. The DEWMA control chart aids in the rapid detection of parameter changes and minor shifts in autocorrelated data.

Due to their ability to manage risk in a variety of situations, time series modeling and forecasting are essential tools used in many areas, including environmental, economic, and financial trends [13]. As a result, understanding statistical methods and time series modeling is crucial for characterizing changes in various processes. Autocorrelation in time series has been studied for a long time, and in a variety of situations, time-series models have been used to predict the data. The data's seasonality and trend were factors. The three main categories are autoregressive (AR), moving average (MA), and autoregressive moving average (ARMA). The data in a time series may exhibit trends or seasonality in some circumstances, such as seasonal autoregressive (SAR), Seasonal moving average (SMA), autoregressive with trends (trend AR), etc. These models of time series were utilized in statistical process control, which in this study used the seasonal model.

An indicator of a control chart's effectiveness is the average run length (ARL). The number of average observations that must remain within the control limit before the procedure alerts that they are out of control is referred to as the ARL. It is split into two categories: ARL_0 (a process is in-control and the values should be high) and ARL_1 (a process is out-of-control and the values should be as small as necessary). The Markov Chain Approach, the Monte Carlo Method, and the Numerical Integral Equation were the techniques that were used in much earlier research to estimate the ARL. They were found in Runger and Prabhu [14], Riaz et al. [15], Karoon et al. [16], and Suriyakat and Petcharat [17]. In addition, explicit formulas are one of the techniques. Many researchers are

interested in using ARLs to measure their effectiveness because explicit formulas can significantly reduce computing time. The ARL of random observations from an MA process with exponential white noise operating on the CUSUM control chart was explicitly formulated by Petcharat et al. [18] in their publication. Sunthornwat et al. [19] provided explicit formulations for the analytical ARL on the EWMA control chart with a long-memory ARFIMA process and contrasted them with the NIE technique. When the data are the first- and general-order autoregressive models with exponential white noise. Phanthuna et al. [20] mentioned that observations of trend-stationary autoregressive operating on the MEWMA control chart resulted in exact formulations of the ARL. Later, Karoon et al. [21–22] proposed explicit formulas for the ARL on the EEWMA control chart based on the first-order and general autoregressive models and compared them with the EWMA and CUSUM control charts, and they found that the EEWMA control chart can be well performed. Recently, the explicit formula of ARL for the EEWMA control chart was derived based on the observations from the quadratic trend AR(p) model, which was proposed by Karoon et al. [23] in 2023. When the data were from an ARMA with an explanatory variables model, Silpakob et al. [24] showed the precise solution of the ARL on a modified EWMA control chart. At the same time, ARL, which runs on a double EWMA control chart, was modified by Karoon et al. [25] to incorporate the use of an explicit approach based on the time series shown in the AR model.

Furthermore, numerous research studies have investigated the modeling of time series using the seasonal model, which has been investigated in many studies and has been widely used in conjunction with the control chart. For example, The MEWMA control chart based on the seasonal autoregressive model and its applications with the percentages of internet users by business and news website categories in Thailand was provided by Phanthuna and Areepong [26]. Phanyaem [27] presented explicit formulas and four numerical integral equation ARL methods based on a seasonal ARX model and the CUSUM control chart. Later, Petcharat [28] improved the explicit ARL formula on the CUSUM control chart. It was running based on the seasonal autoregressive with trend model, utilizing the Fredholm integral equation technique, and afterwards applied actual data to the silver price data. The exact formula of ARL that operates on an extended EWMA control chart and runs underlying the seasonal AR model was presented by Karoon et al. [29]. They enlarged it to assess the effectiveness of regular EWMA control charts and then used real data, the number of internet users, to confirm the conclusions of these. Chananet and Phanyaem [30] developed the explicit formula for ARL based on the CUSUM control chart. It uses observations from a seasonal AR model with exogenous variables. They further developed it to contrast the ARL of CUSUM generated by NIE with Gaussian and midpoint rules. Later, Petcharat [31] proposed the ARL that was obtained by an exact solution running on the EWMA control chart under the seasonal MAX model, compared it to the NIE with Gaussian and Midpoint rules, and extended it to compare with the CUSUM control chart.

In addition to the aforementioned, seasonal time-series models are useful in a variety of applications. Chen and Wang presented the seasonal ARIMA model in 2007 [32], which

was used to anticipate the production values of the equipment sector. Montaser et al. [33] presented the performance of a seasonal model based on ARIMA for applications in glucose prediction in an artificial pancreas. As shown by Kadri et al. in 2019 [34], a seasonal ARMA model was employed to predict the emergency department systems.

However, the explicit ARL of the DEWMA control chart based on the data is a seasonal autoregressive model that has not been done before. Using the DEWMA control chart, this paper's main objective is to construct explicit ARL formulae for the data and compare them to the NIE method, which uses seasonal autoregressive models. Then, for both simulated and real data, the DEWMA control chart is extended for comparison to the EWMA control chart. Its applications are about O_3 and PM10 in Chiang Mai, Thailand; those are important pollutants.

II. MATERIALS AND METHODS

In this section, we present the DEWMA statistic design along with data from the seasonal autoregressive model $(SAR(p)_s)$, followed by the explicit formula and NIE approach of the ARL.

A. The DEWMA Control Chart

First of all, Robert is credited with coming up with the EWMA control chart [6]. It typically tracks and finds minute variations in the process's mean. The equation below can be employed to describe the statistics of the EWMA control chart in (1).

$$Z_t = \lambda X_t + (1-\lambda)Z_{t-1} \qquad (1)$$

where the EWMA control chart parameter X_t is a sequence of seasonal autoregressive $(SAR(p)_s)$ model and a sequence data at $t = 1, 2, 3, ...$ with exponential white noise, λ is an exponential smoothing parameter $(0,1]$, X_t at $t = 0$ is the initial value of the EWMA statistics. Its mean is equal to μ and variance of X_t is equal to $\lambda\sigma^2/(2-\lambda)$. And then, the upper control limit (UCL) and lower control limit (LCL) can be described from the mean μ, the standard deviation σ, and a control width limit B as follows:

$$UCL = \mu + B\sigma\sqrt{\frac{\lambda}{2-\lambda}}, LCL = \mu - B\sigma\sqrt{\frac{\lambda}{2-\lambda}}.$$

The EWMA control chart's stopping time is written as:
$$\tau_b = \inf\{t \geq 0 : Z_t > UCL\}.$$

Second, Mahmoud and Woodall [11] improved the DEWMA control chart after Shamma and Shamma initially proposed it in 1992 [12]. It was extended from the EWMA control chart after being smoothed twice exponentially. The equation in (2) below could be used to describe the statistics of the DEWMA control chart.

$$DE_t = \lambda_2 Z_t + (1-\lambda_2)DE_{t-1}$$
$$Z_t = \lambda_1 X_t + (1-\lambda_1)Z_{t-1}. \qquad (2)$$

where the DEWMA control chart parameter X_t is a sequence of seasonal autoregressive $(SAR(p)_s)$ model and a sequence data at $t = 1, 2, 3, ...$ with exponential white noise, λ_1 and λ_2 are exponential smoothing parameters equals

$(0,1]$, X_t at $t = 0$ is the initial value of the DEWMA statistics. Its mean is equal to μ and variance of X_t is equal to $\frac{\lambda_1^2 \lambda_2^2}{(\lambda_1 - \lambda_2)^2} \sigma^2 \left[\frac{(1-\lambda_2)^2}{1-(1-\lambda_2)^2} + \frac{(1-\lambda_1)^2}{1-(1-\lambda_1)^2} - 2\frac{(1-\lambda_1)(1-\lambda_2)}{1-(1-\lambda_1)(1-\lambda_2)} \right]$.

And then, the upper control limit (*UCL*) and lower control limit (*LCL*) can be described from the mean μ, the standard deviation σ, and a control width limit *D* as follows:

$$UCL = \mu + D\sigma \sqrt{\frac{\lambda_1^2 \lambda_2^2}{(\lambda_1 - \lambda_2)^2} \left[\frac{(1-\lambda_2)^2}{1-(1-\lambda_2)^2} + \frac{(1-\lambda_1)^2}{1-(1-\lambda_1)^2} - 2\frac{(1-\lambda_1)(1-\lambda_2)}{1-(1-\lambda_1)(1-\lambda_2)} \right]},$$

$$LCL = \mu - D\sigma \sqrt{\frac{\lambda_1^2 \lambda_2^2}{(\lambda_1 - \lambda_2)^2} \left[\frac{(1-\lambda_2)^2}{1-(1-\lambda_2)^2} + \frac{(1-\lambda_1)^2}{1-(1-\lambda_1)^2} - 2\frac{(1-\lambda_1)(1-\lambda_2)}{1-(1-\lambda_1)(1-\lambda_2)} \right]}.$$

The EWMA control chart's stopping time is written as:

$$\tau_b = \inf\{t \geq 0 : DE_t > UCL\}.$$

Moreover, if λ_1 equals 1 in the DEWMA statistic, that becomes the EWMA statistic.

B. The DEWMA Control Chart for SAR(p)ₛ Models

Monitoring industrial operations, the environment, the provision of healthcare, and the tracking of corporate financial indicators all require the use of time series data. Data points collected over time may contain internal structures (such as autocorrelation, trend, or seasonal fluctuation) that need to be taken into consideration. Time-series analysis takes this into account. Many time series have seasonal activity, with fundamental patterns that recur seasonally across time. A seasonal model can also be defined using different metrics, such as autoregressive (AR(p)), moving average (MA(q)), autoregressive moving average (ARMA(p,q)), and so on. In this article, we looked at the seasonal autoregressive model, also known as the SAR(p)ₛ model.

The seasonal autoregressive model for lag p and period s of the seasonality, denoted by SAR(p)ₛ, is written in (3) as:

$$X_t = c + \phi_1 X_{t-1s} + \phi_2 X_{t-2s} + ... + \phi_p X_{t-ps} + \varepsilon_t \qquad (3)$$

Where $\varepsilon_t \sim Exp(\beta)$

X_t is a sequence from a SAR(p)ₛ model,

c is the constant of the model,

$\phi_1, \phi_2, ..., \phi_p$ are coefficients of the seasonal autoregressive model with values of $|\phi_p| < 1$,

s is the number of seasonal periods (e.g., s equals 4 for quarterly data and s equals 12 for monthly data),

ε_t is the error terms for white noise exponential distribution,

and, $X_{t-1s}, X_{t-2s}, ..., X_{t-ps}$ are initial values with the process mean.

For the DEWMA control chart running a seasonal autoregressive model, the initial value of ARL denoted $D(\varpi)$ and the initial value of the monitoring DEWMA statistic $DE_0 = \varpi$ represented at $\varpi \in [0,b]$. As the result, the function $D(\varpi)$ is defined in (4) as follows:

$$ARL = D(\varpi) = E_\infty(\tau_b) \qquad (4)$$

The following definitions apply to the ARL in (4):

$$ARL = D(\varpi) = \begin{cases} ARL_0 = E_\infty(\tau_b), & (no \quad change), \quad in-control \\ ARL_1 = E_1(\tau_b), & (change), \quad out-of-control \end{cases},$$

where $E_\infty(\cdot)$ denote the expectation with the density function as $f(x, \beta)$. After that, it can be used in the following section about process monitoring. The change-point models are considered as follows:

$$\varepsilon_t \sim \begin{cases} Exp(\beta_0), & t = 1, 2, 3, ..., \theta - 1 \\ Exp(\beta_1), & t = \theta, \theta + 1, \theta + 2, ... \end{cases}.$$

Herein, $\theta = \infty$ is known as the in-control ARL (ARL₀) and denotes that there has been no change in the statistical control process. On the other hand, $\theta = 1$ denotes the first time point in the statistical control process when a change occurs from β_0 to β, which is referred to an out-of-control ARL (ARL₁).

C. Explicit Formula and NIE for SAR(p)ₛ Models
Analytical Explicit Formula of the ARL

This part uses a seasonal autoregressive model with an exponential noise distribution to solve the analytically explicit formula of the ARL on the DEWMA control chart. It is assumed that the lower control limit (*LCL*) is equal to 0 and the upper control limit (*UCL*) is equal to *b*.

First, solve the seasonal autoregressive (SAR(p)ₛ) explicit formula for the ARL operating on the DEWMA control chart. The SAR(p)ₛ model is used as X_t in (3) instead of the DEWMA statistics in (2), in the following:

$$DE_t = \lambda_1 \lambda_2 \left(c + \phi_1 X_{t-1s} + \phi_2 X_{t-2s} + ... + \phi_p X_{t-ps} + \varepsilon_t \right) + \lambda_2(1-\lambda_1)Z_{t-1} + (1-\lambda_2)DE_{t-1}.$$

$DE_{t-1} = \varpi$ is supported by the first point in time at $t = 1$, and the initial value of the DEWMA statistic Z₀ is equal to Ω. In terms of SAR(p)ₛ, the DEWMA statistic is as follows:

$$DE_1 = \lambda_1 \lambda_2 \left(c + \phi_1 X_{t-1s} + \phi_2 X_{t-2s} + ... + \phi_p X_{t-ps} + \varepsilon_1 \right) + \lambda_2(1-\lambda_1)\Omega + (1-\lambda_2)\varpi.$$

Second, solve the error term. The range of DE_1 between the lower and upper bound control limits is stated in the control process as 0 to *b* and the error term ε_1 may be expressed as follows: $n < \varepsilon_1 < n^*$. $\qquad (5)$

Where n represents $\frac{0 - (1-\lambda_2)\varpi}{\lambda_1 \lambda_2} - \frac{(1-\lambda_1)\Omega}{\lambda_1} - \left(c + \sum_{i=1}^{p} \phi_i X_{t-is} \right)$

and n^* represents $\frac{b - (1-\lambda_2)\varpi}{\lambda_1 \lambda_2} - \frac{(1-\lambda_1)\Omega}{\lambda_1} - \left(c + \sum_{i=1}^{p} \phi_i X_{t-is} \right)$,

respectively.

Third, solve the ARL by using the Fredholm integral equation of the second kind [35]. The equation is shown as follows:

$$D(\varpi) = \int_n^{n^*} D\left(\lambda_1 \lambda_2 \left(c + \sum_{i=1}^{p} \phi_i X_{t-is} + \varepsilon_1 \right) + \lambda_2(1-\lambda_1)\Omega + (1-\lambda_2)\varpi \right) \cdot f(\omega) d\omega,$$

Then, when the integration variable is substituted to get

$$\omega = \lambda_1 \lambda_2 \left(c + \sum_{i=1}^{p} \phi_i X_{t-is} + \varepsilon_1 \right) + \lambda_2(1-\lambda_1)\Omega + (1-\lambda_2)\varpi,$$

$D(\varpi)$ has been rearranged as follows:

$$D(\varpi) = 1 + \frac{1}{\lambda_1 \lambda_2} \int_0^b D(\omega) f \left(\frac{\omega - (1-\lambda_2)\varpi}{\lambda_1 \lambda_2} - \frac{(1-\lambda_1)\Omega}{\lambda_1} - \sum_{i=1}^p \phi_i X_{t-is} - c \right) d\omega. \quad (6)$$

Next, the error terms then describe the function $D(\varpi)$ as an exponential distribution function. So, the function $D(\varpi)$ is rewritten as:

$$D(\varpi) = 1 + \frac{1}{\beta \lambda_1 \lambda_2} e^q \int_0^b D(\omega) \cdot e^{\frac{-\omega}{\beta \lambda_1 \lambda_2}} d\omega. \quad (7)$$

where $q = \frac{(1-\lambda_2)\varpi}{\beta \lambda_1 \lambda_2} + \frac{(1-\lambda_1)\Omega}{\beta \lambda_1} + \frac{\lambda_1 \lambda_2}{\beta}(c + \sum_{i=1}^p \phi_i X_{t-is})$,

$G(\varpi) = e^q$.

After that, the explicit formula ARL, which is running on the DEWMA control chart based on the SAR(p)$_s$ model, is then checked for existence and uniqueness using Equation (7), and the solution is found using Banach's fixed point theorem [36].

Theorem1: Banach's fixed point theorem

Let (X, d) represent a complete metric space and Let $T : X \to X$ represent the contraction mapping. And then, T denote unique on fixed point. There exists a unique solution to the fixed point when $T(\varpi) = \varpi$.

To proof that, let T determined in Eq. (6) is a contraction mapping for $D(\varpi)_1, D(\varpi)_2 \in G[0, b]$. Such that,

$$\| T(D(\varpi)_1) - T(D(\varpi)_2) \| \le h \| D(\varpi)_1 - (D(\varpi)_2 \|,$$

$$D(\varpi)_1, D(\varpi)_2 \in X,$$

where h denotes a positive constant.

Therefore,

$$\| TD(\varpi)_1) - T(D(\varpi)_2) \|_\infty = \sup_{\varpi \in [0,b]} |(D(\varpi)_1 - (D(\varpi)_2|$$

$$= \sup_{\varpi \in [0,b]} \left| \frac{1}{\beta \lambda_1 \lambda_2} e^q \int_0^b (D(\omega)_1 - D(\omega)_2) \cdot e^{\frac{-\omega}{\beta \lambda_1 \lambda_2}} d\omega \right|$$

$$\le \sup_{\varpi \in [0,b]} \frac{1}{\beta \lambda_1 \lambda_2} e^q \left| \int_0^b e^{\frac{-\omega}{\beta \lambda_1 \lambda_2}} d\omega \right| \| D(\omega)_1 - D(\omega)_2 \|_\infty$$

$$\le \sup_{\varpi \in [0,b]} \left\{ e^q \cdot \left(1 - e^{\frac{-b}{\beta \lambda_1 \lambda_2}} \right) \right\} \cdot \| D(\omega)_1 - D(\omega)_2 \|_\infty$$

$$\le h \| D(\omega)_1 - D(\omega)_2 \|_\infty, \text{ where } h \in [0,1) .$$

The explicit ARL is simplified to give a uniqueness and existence solution.

After checking for uniqueness and existence, the next step is setting new variables in equation (7), which can be presented as follows:

$$\eta = \int_0^b D(\omega) \cdot e^{\frac{-\omega}{\beta \lambda_1 \lambda_2}} d\omega .$$

Therefore, by adding new variables, the explicit ARL solution can be rewritten as follows:

$$D(\varpi) = 1 + \frac{1}{\beta \lambda_1 \lambda_2} G(\varpi) \cdot \eta . \quad (8)$$

Next step, Equation (8) is used instead of $D(\varpi)$, Its procedure is illustrated below.

From $\quad \eta = \int_0^b D(\omega) \cdot e^{\frac{-\omega}{\beta \lambda_1 \lambda_2}} d\omega$,

we will get $\quad \eta = \int_0^b (1 + \frac{1}{\beta \lambda_1 \lambda_2} G(\omega) \cdot \eta) \cdot e^{\frac{-\omega}{\beta \lambda_1 \lambda_2}} d\omega .$

Such that,

$$\eta = \frac{-\beta \lambda_1 \lambda_2 \left[1 - e^{\frac{-b}{\beta \lambda_1 \lambda_2}} \right]}{1 + \frac{1}{\lambda_2} \cdot e^{\frac{c + \sum_{i=1}^p \phi_i X_{t-is}}{\beta} + \frac{(1-\lambda_1)\Omega}{\beta \lambda_1}} \cdot \left[1 - e^{\frac{-b}{\beta \lambda_1}} \right]} . \quad (9)$$

After that, η in (9) is substituted into (8), the $D(\varpi)$ can be rewritten as:

$$D(\varpi) = 1 - \frac{\lambda_2 e^{\frac{(1-\lambda_2)\varpi}{\beta \lambda_1 \lambda_2}} \cdot \left[1 - e^{\frac{-b}{\beta \lambda_1 \lambda_2}} \right]}{\lambda_2 e^{\frac{c + \sum_{i=1}^p \phi_i X_{t-is}}{\beta} + \frac{(1-\lambda_1)\Omega}{\beta \lambda_1}} + \left[1 - e^{\frac{-b}{\beta \lambda_1}} \right]} . \quad (10)$$

So, the explicit ARL solution on the DEWMA control chart for the model of data is SAR(p)$_s$, which is shown in (10). Moreover, the explicit ARL$_0$ (the in-control circumstance) in $D(\varpi)$ is obtained by $\beta = \beta_0$ in (10) whereas the explicit ARL$_1$ (the out-of-control circumstance) in $D(\varpi)$ in obtained by $\beta = \beta_1$ in (10), and then $\beta_1 = \beta_0(1+\delta)$.

Analytical NIE of the ARL

The NIE approach could be used to calculate the ARL of the SAR(p)$_s$ model running on the DEWMA control chart. Let $D(\varpi)^*$ be the ARL of the NIE approach on the DEWMA control chart when the model of the data is SAR(p)$_s$. The ARL of the NIE approach is estimated by starting from (8) and computing in terms of the m linear equation systems with the midpoint rule on the interval $[0,b]$. The interval is subdivided into m subintervals ($[y_{k-1}, y_k]$, $k=1,2,...,m$), a set of equal width ($d_j = b/m$), and the intermediate value of the kth interval to be $y_j = d_j(j - 0.5)$.

The quadrature rule evaluates the estimation for an integral in (11) as follows:

$$\int_0^b D(\omega) f(\omega) d\omega \approx \sum_{j=1}^m d_j f(y_j) \quad (11)$$

The NIE approach ($D(\varpi)^*$), which is approximated by a linear equation, has a solution, as follows below.

$$D(y_i)^* = 1 + \frac{1}{\lambda_1 \lambda_2} \sum_{j=1}^m d_j D(y_j) \cdot f \left(\frac{y_j - (1-\lambda_2)y_i}{\lambda_1 \lambda_2} - \frac{(1-\lambda_1)\Omega}{\lambda_1} - c - \sum_{i=1}^p \phi_i X_{t-is} \right),$$

$i = 1, 2, ..., m$

Finally, substituting ϖ for y_i in $D(y_i)^*$, the solution of the NIE approach for the function $D(\varpi)$ being expressed as the function $D(\varpi)^*$ in (12) as follows:

$$D(\varpi)^* = 1 + \frac{1}{\lambda_1 \lambda_2} \sum_{j=1}^{m} d_j D(y_j) \cdot f \left(\begin{array}{c} \dfrac{y_j - (1-\lambda_2)\varpi}{\lambda_1 \lambda_2} - \dfrac{(1-\lambda_1)\Omega}{\lambda_1} \\ -c - \sum_{i=1}^{p} \phi_i X_{t-is} \end{array} \right) .(12)$$

where $y_j = d_j(j - 0.5)$ and $d_j = b/m$, $j = 1, 2, \ldots, m$.

III. EFFICIENCY COMPARISON AND EVALUATION OF ARL

A. Experimental Results of ARL

This section examined the explicit ARL using the Fredholm integral equation and contrasted it with the ARL of the NIE technique using the Gauss-Legendre quadrature rule as well as the composite midpoint rule based on the DEWMA control chart with 1,000 division nodes. A seasonal autoregressive $(SAR(p)_s)$ model was used to analyze the experimental data. The Mathematica software calculated the codes for computing the explicit ARL and the NIE method of the ARL. The accuracy of the ARL that approximates values is measured by the relative error (%RE). The ARL's expressly created formulas checked the performance's effectiveness in terms of the relative error (%RE) and computation time. That is calculated following the equation below.

$$\%RE = \left| \frac{D(\varpi) - D(\varpi)^*}{D(\varpi)} \right| \times 100\% \qquad (13)$$

where $D(\varpi)$ and $D(\varpi)^*$ are the explicit ARL in (10) and the ARL of the NIE technique in (12), respectively.

The simulated data is commonly provided with $ARL_0 = 370$ for the in-control circumstance, allowing the starting parameters to be studied at $\beta_0 = 1$, whereas β_1 is investigated in the out-of-control circumstance and computed at determining small and modulate shift (δ), such as 0.001, 0.002, 0.003, 0.004, 0.005, 0.01, 0.02, 0.05, and 0.5. And then the lower and upper control limits are studied for the exponential distribution at the interval [0, b]. The one-sided DEWMA structure of the explicit ARL values was associated with $SAR(1)_{12}$ and $SAR(2)_{12}$ models.

The simulated data of $SAR(1)_{12}$ with and $SAR(2)_{12}$ models are shown in Table I. and II. Those were compared to the ARL values of the NIE technique. The results in Table I. and Table II. were showed the performance of the explicit ARL against the ARL of the NIE techniques. Results from the explicit ARL are comparable to those from the NIE methodology; however, the computational durations for the explicit ARL's significant relative error times are instantaneous, whereas those for the NIE method's ARL are between 7-9 seconds.

B. Performance Comparison of the Explicit ARL

This section investigated the explicit ARL with the DEWMA control chart using different λ_1 values and compared its capability to the EWMA control chart using λ_1 equals 1. The exponential smoothing parameters are set small (λ_2 equals 0.05 and 0.1) and moderate (λ_2 equals 0.2 and 0.3) on the $SAR(1)_{12}$ and the $SAR(2)_{12}$ models.

TABLE I
THE EXPLICIT ARL VALUES AGAINST THE ARL VALUES OF THE NIE METHOD ON THE DEWMA CHART WITH THE DATA RUNNING ARE $SAR(1)_{12}$.

δ		$\lambda_1 = 0.05$	
		$\lambda_1 = \lambda_2,$ $\phi_1 = 0.2$ $b = 0.0003669357$	$4\lambda_1 = \lambda_2,$ $\phi_1 = -0.2$ $b = 0.001545667$
0	$D(\varpi)$	370.01453428 (<0.001)	370.04734182 (<0.001)
	$D(\varpi)^*$	370.01453363 (7.765)	370.04733569 (7.890)
	%RE	0.00000018	0.00000166
0.001	$D(\varpi)$	172.12999928 (<0.001)	174.50987343 (<0.001)
	$D(\varpi)^*$	172.12999905 (7.985)	174.50987199 (7.875)
	%RE	0.00000013	0.00000083
0.002	$D(\varpi)$	112.35093284 (<0.001)	114.37383494 (<0.001)
	$D(\varpi)^*$	112.35093272 (7.923)	114.37383429 (7.921)
	%RE	0.00000012	0.00000057
0.003	$D(\varpi)$	83.49985789 (<0.001)	85.16994582 (<0.001)
	$D(\varpi)^*$	83.49985780 (7.906)	85.16994543 (7.860)
	%RE	0.00000011	0.00000045
0.004	$D(\varpi)$	66.50780220 (<0.001)	67.91469329 (<0.001)
	$D(\varpi)^*$	66.50780213 (7.922)	67.91469304 (7.938)
	%RE	0.00000010	0.00000037
0.005	$D(\varpi)$	55.30949921 (<0.001)	56.52039143 (<0.001)
	$D(\varpi)^*$	55.30949916 (7.984)	56.52039124 (7.953)
	%RE	0.00000010	0.00000033
0.01	$D(\varpi)$	30.23673288 (<0.001)	30.94359335 (<0.001)
	$D(\varpi)^*$	30.23673285 (7.999)	30.94359329 (7.875)
	%RE	0.00000009	0.00000021
0.02	$D(\varpi)$	16.14112652 (<0.001)	16.52488538 (<0.001)
	$D(\varpi)^*$	16.14112651 (7.969)	16.52488536 (8.077)
	%RE	0.00000008	0.00000015
0.05	$D(\varpi)$	7.11166453 (<0.001)	7.27328790 (<0.001)
	$D(\varpi)^*$	7.11166452 (7.937)	7.27328789 (7.953)
	%RE	0.00000007	0.00000010
0.5	$D(\varpi)$	1.51663432 (<0.001)	1.53340793 (<0.001)
	$D(\varpi)^*$	1.51663432 (7.876)	1.53340793 (7.891)
	%RE	0.00000001	0.00000002

Note: The results in parentheses are the computational times in seconds

TABLE II
THE EXPLICIT ARL VALUES AGAINST THE ARL VALUES OF
THE NIE METHOD ON THE DEWMA CHART WITH THE DATA
RUNNING ARE SAR(2)$_{12}$.

δ		$\lambda_1 = 0.1$	
		$\lambda_1 = \lambda_2,$ $\phi_1 = 0.3$ $b = 0.003935012$	$2\lambda_1 = \lambda_2,$ $\phi_1 = -0.3$ $b = 0.00854954$
0	$D(\varpi)$	370.07317709 (<0.001)	370.03645639 (<0.001)
	$D(\varpi)*$	370.07316428 (8.219)	370.03640473 (8.280)
	%RE	0.00000346	0.00001396
0.001	$D(\varpi)$	200.83279025 (<0.001)	205.45992145 (<0.001)
	$D(\varpi)*$	200.83278591 (8.375)	205.45990494 (8.218)
	%RE	0.00000216	0.00000804
0.002	$D(\varpi)$	138.00219472 (<0.001)	142.39721552 (<0.001)
	$D(\varpi)*$	138.00219241 (8.297)	142.39720731 (8.250)
	%RE	0.00000167	0.00000577
0.003	$D(\varpi)$	105.22749104 (<0.001)	109.06392275 (<0.001)
	$D(\varpi)*$	105.22748955 (8.265)	109.06391777 (8.265)
	%RE	0.00000142	0.00000457
0.004	$D(\varpi)$	85.10487553 (<0.001)	88.44732723 (<0.001)
	$D(\varpi)*$	85.10487446 (8.297)	88.44732385 (8.312)
	%RE	0.00000126	0.00000382
0.005	$D(\varpi)$	71.49346977 (<0.001)	74.43602753 (<0.001)
	$D(\varpi)*$	71.49346894 (8.359)	74.43602506 (8.265)
	%RE	0.00000116	0.00000331
0.01	$D(\varpi)$	39.95781567 (<0.001)	41.76811381 (<0.001)
	$D(\varpi)*$	39.95781531 (8.266)	41.76811292 (8.343)
	%RE	0.00000090	0.00000213
0.02	$D(\varpi)$	21.55271193 (<0.001)	22.56812959 (<0.001)
	$D(\varpi)*$	21.55271178 (8.220)	22.56812927 (8.265)
	%RE	0.00000074	0.00000141
0.05	$D(\varpi)$	9.49069606 (<0.001)	9.93098564 (<0.001)
	$D(\varpi)*$	9.49069600 (8.297)	9.93098555 (8.296)
	%RE	0.00000058	0.00000088
0.5	$D(\varpi)$	1.848654363 (<0.001)	1.900194303 (<0.001)
	$D(\varpi)*$	1.848654361 (8.218)	1.900194300 (7.891)
	%RE	0.00000013	0.00000017

Note: The results in parentheses are the computational times in seconds

The results for contrasting capability between the DEWMA and EWMA control charts based on different situations are shown in Table III. and IV and Fig. 1. and 2.

The results showed that the DEWMA control chart received lower ARL1 values than the EWMA control chart in all situations. The DEWMA control chart with $\lambda_1 = 0.5\lambda_2$ also outperformed the DEWMA control chart with $\lambda_1 = \lambda_2$ and $\lambda_1 = 2\lambda_2$ and the EWMA control chart, respectively, for both SAR(1)$_{12}$ and SAR(2)$_{12}$ models in all cases. Correspondingly, the relative mean index (RMI), a measurement, may also be used to confirm the effectiveness of each control chart [37]. The RMI in (14) is calculated as follows:

$$RMI = \frac{1}{n} \sum_{i=1}^{n} \frac{ARL_i - ARL_i^*}{ARL_i^*} \tag{14}$$

where the ARL value for row i^{th} on the tested control chart is ARL_i, and the lowest ARL value for row i^{th} on the tested control chart is ARL_i^*. The control chart, this one, can be given the lowest RMI value and has more capability than other control charts. Additionally, the average extra quadratic loss (AEQL) is a metric that may be used to assess the effectiveness of each control chart [38]. The AEQL is calculated in (15) as follows:

$$AEQL = \frac{1}{\Delta} \sum_{\delta_i = \delta_{\min}}^{\delta_{\max}} \left(\delta_i^2 \times ARL(\delta_i) \right) \tag{15}$$

where δ_i is the amount of shift in the operation calculated by the control chart, $ARL(\delta_i)$ is the ARL value of the control chart for the amount of shift δ_i, and Δ is the sum of shift numbers from $\delta_{\min}$ to $\delta_{\max}$. In this study, Δ was determined as 10 increments from $\delta_{\min} = 0$ to $\delta_{\max} = 0.5$. The control chart can be given the lowest AEQL value and has more capability than other control charts, for which the criteria are indicated similarly to the RMI measurement. The results shown are the RMI and AEQL values of the DEWMA and EWMA charts based on different parameters to confirm the performance of the control charts as presented in Table V. The results show the RMI and AEQL values of each control charts; the DEWMA chart with $\lambda_1 = 0.5\lambda_2$ has the lowest RMI and AEQL values for all cases. So, the DEWMA chart outperforms the EWMA chart with all of its different λ in every situation. The exponential smoothing parameters λ_2 are so low that the performance of the DEWMA control chart is good. Note that, the bold in Table V is the lowest RMI and AEQL values when the values were compared by using different λ_1 of the DEWMA and EWMA charts, and DEWMA_05, DEWMA_1, DEWMA_2 in Figs. 1, 2, 4, and 5 are instead of DEWMA with $\lambda_1 = 0.5\lambda_2$, $\lambda_1 = \lambda_2$, and $\lambda_1 = 2\lambda_2$, respectively.

TABLE III

PERFORMANCE COMPARISON ON THE DEWMA (DIFFERENT λ PARAMETERS WERE GIVEN) AND EWMA CONTROL CHARTS, AND DIFFERENT SHIFT SIZES IN THE MODEL WERE PERFORMED WITH SAR(1)$_{12}$ AND DETERMINED COEFFICIENT MODEL (ϕ_1) EQUAL TO 0.2.

λ_2	Control Charts	λ_1	b	Shift sizes (δ)									
				0	0.001	0.002	0.003	0.004	0.005	0.01	0.02	0.05	0.5
0.05	DEWMA	$\lambda_1 = 0.5\lambda_2$	0.00002474721	370	130.92	79.74	57.44	44.96	36.97	19.77	10.49	4.69	1.22
		$\lambda_1 = \lambda_2$	0.0003669357	370	172.13	112.35	83.50	66.51	55.31	30.24	16.14	7.11	1.52
		$\lambda_1 = 2\lambda_2$	0.002008143	370	200.59	137.78	105.03	84.94	71.35	39.87	21.51	9.48	1.85
	EWMA	$\lambda_1 = 1$	0.05016143	370	236.37	173.84	137.58	113.91	96.42	56.43	31.07	13.78	2.48
0.1	DEWMA	$\lambda_1 = 0.5\lambda_2$	0.000736578	370	172.57	112.72	83.80	66.76	55.53	30.36	16.21	7.14	1.52
		$\lambda_1 = \lambda_2$	0.004057362	370	201.82	138.94	106.05	85.82	72.12	40.34	21.77	9.59	1.86
		$\lambda_1 = 2\lambda_2$	0.01356398	370	220.39	157.10	122.17	100.02	84.72	48.26	26.29	11.61	2.16
	EWMA	$\lambda_1 = 1$	0.10296968	370	239.89	177.64	141.14	117.16	100.20	58.39	32.22	14.29	2.54
0.2	DEWMA	$\lambda_1 = 0.5\lambda_2$	0.008286	370	204.38	141.36	108.15	87.65	73.73	41.33	22.32	9.82	1.88
		$\lambda_1 = \lambda_2$	0.02811368	370	224.83	161.65	126.29	103.70	88.02	50.36	27.50	12.14	2.21
		$\lambda_1 = 2\lambda_2$	0.07376465	370	237.86	175.42	139.04	115.24	98.44	57.20	31.50	13.94	2.46
	EWMA	$\lambda_1 = 1$	0.2177584	370	247.30	185.85	148.96	124.35	106.78	62.82	34.84	15.46	2.66
0.3	DEWMA	$\lambda_1 = 0.5\lambda_2$	0.02731528	370	221.25	157.97	122.94	100.70	85.32	48.62	26.47	11.66	2.13
		$\lambda_1 = \lambda_2$	0.07934069	370	239.02	176.66	140.21	116.30	99.40	57.83	31.85	14.08	2.45
		$\lambda_1 = 2\lambda_2$	0.1925868	370	250.19	189.12	152.11	127.28	109.46	64.65	35.92	15.93	2.69
	EWMA	$\lambda_1 = 1$	0.347435	370	255.33	195.04	157.87	132.66	114.45	68.11	38.01	16.88	2.81

TABLE IV

PERFORMANCE COMPARISON ON THE DEWMA (DIFFERENT λ PARAMETERS WERE GIVEN) AND EWMA CONTROL CHARTS, AND DIFFERENT SHIFT SIZES IN THE MODEL WERE PERFORMED WITH SAR(2)$_{12}$ AND DETERMINED COEFFICIENT MODEL (ϕ_1 AND ϕ_2) EQUAL TO 0.2 AND -0.3, RESPECTIVELY.

| λ_2	Control Charts	λ_1	b	Shift sizes (δ)									
				0	0.001	0.002	0.003	0.004	0.005	0.01	0.02	0.05	0.5
0.05	DEWMA	$\lambda_1 = 0.5\lambda_2$	0.00002550128	370	131.42	80.11	57.72	45.18	37.16	19.88	10.54	4.71	1.22
		$\lambda_1 = \lambda_2$	0.000378155	370	172.90	113.00	84.04	66.96	55.70	30.47	16.27	7.17	1.52
		$\lambda_1 = 2\lambda_2$	0.002069962	370	201.54	138.68	105.82	85.62	71.95	40.25	21.72	9.57	1.87
	EWMA	$\lambda_1 = 1$	0.0517304	370	238.00	175.60	139.23	115.42	98.61	57.34	31.61	14.03	2.52
0.1	DEWMA	$\lambda_1 = 0.5\lambda_2$	0.000759185	370	173.34	113.38	84.35	67.22	55.92	30.60	16.34	7.20	1.53
		$\lambda_1 = \lambda_2$	0.004183598	370	202.83	139.89	106.88	86.54	72.76	40.74	21.99	9.69	1.88
		$\lambda_1 = 2\lambda_2$	0.0139921	370	221.66	158.39	123.33	101.06	85.65	48.85	26.64	11.77	2.18
	EWMA	$\lambda_1 = 1$	0.10628055	370	241.64	179.57	142.98	118.85	101.74	59.42	32.83	14.57	2.57
0.2	DEWMA	$\lambda_1 = 0.5\lambda_2$	0.00854954	370	205.46	142.40	109.06	88.45	74.44	41.77	22.57	9.93	1.90
		$\lambda_1 = \lambda_2$	0.0290356	370	226.26	163.12	127.64	104.91	89.10	51.07	27.91	12.32	2.24
		$\lambda_1 = 2\lambda_2$	0.076240841	370	239.60	177.32	140.85	116.89	99.94	58.21	32.09	14.21	2.50
	EWMA	$\lambda_1 = 1$	0.2252005	370	249.38	188.20	151.23	126.47	108.72	64.15	35.64	15.82	2.70
0.3	DEWMA	$\lambda_1 = 0.5\lambda_2$	0.02823092	370	222.67	159.42	124.25	101.87	86.37	49.29	26.86	11.83	2.15
		$\lambda_1 = \lambda_2$	0.0821211	370	240.86	178.69	142.13	118.06	101.01	58.90	32.49	14.37	2.49
		$\lambda_1 = 2\lambda_2$	0.1995475	370	252.44	191.70	154.61	129.61	111.62	66.14	36.82	16.33	2.74
	EWMA	$\lambda_1 = 1$	0.3601765	370	257.77	197.90	160.70	135.33	116.92	69.84	39.06	17.36	2.87
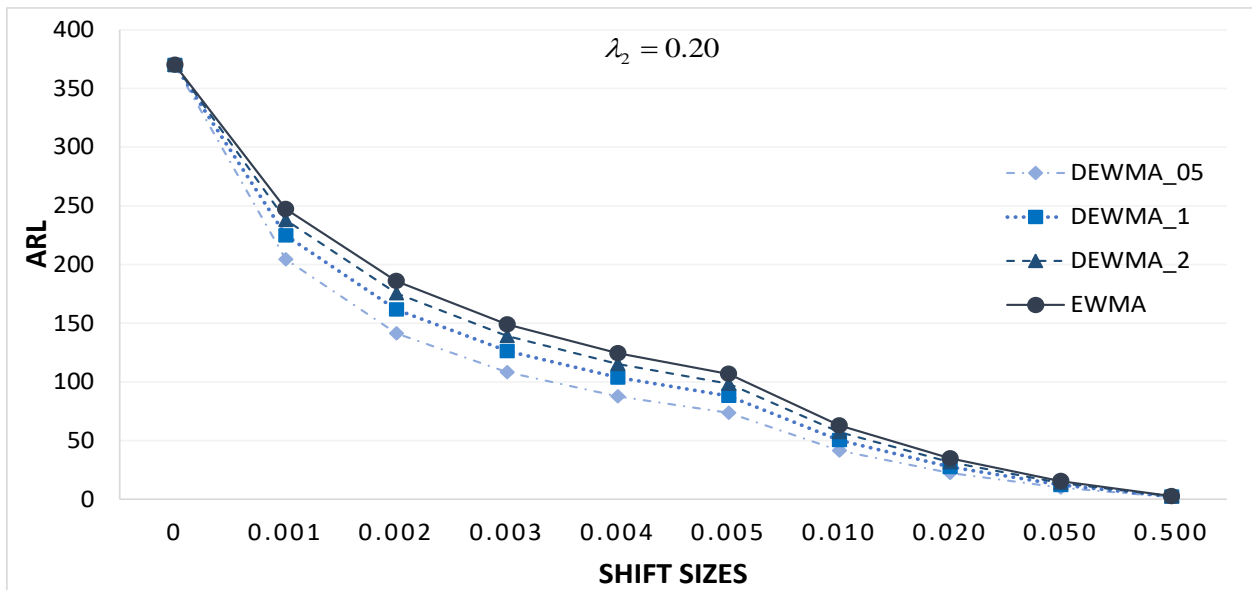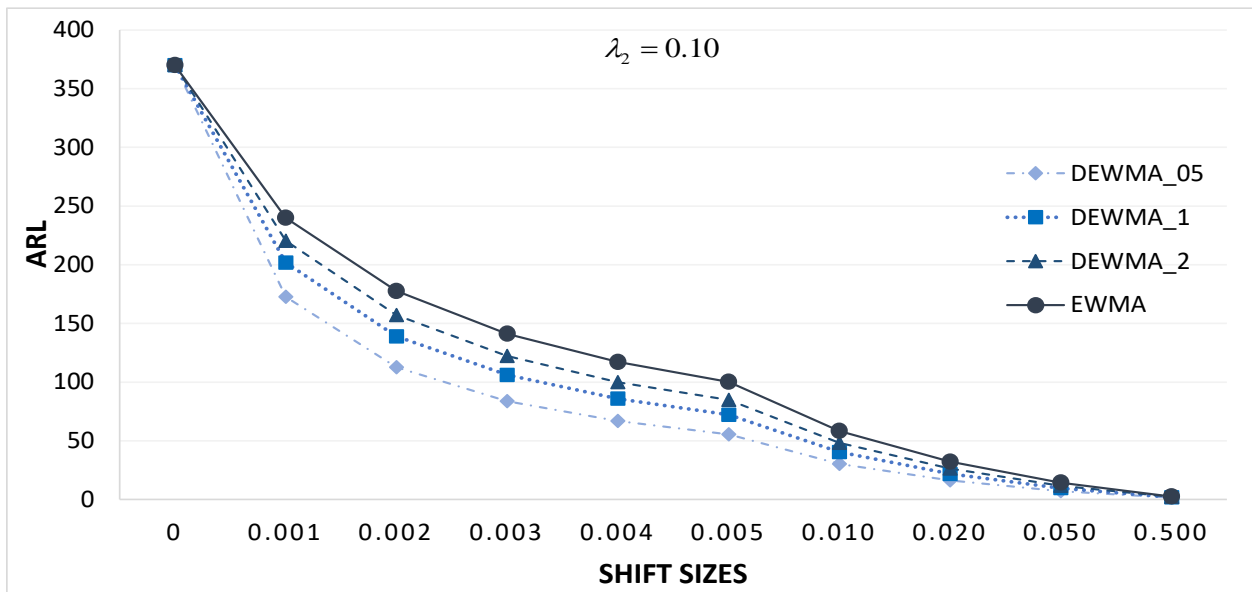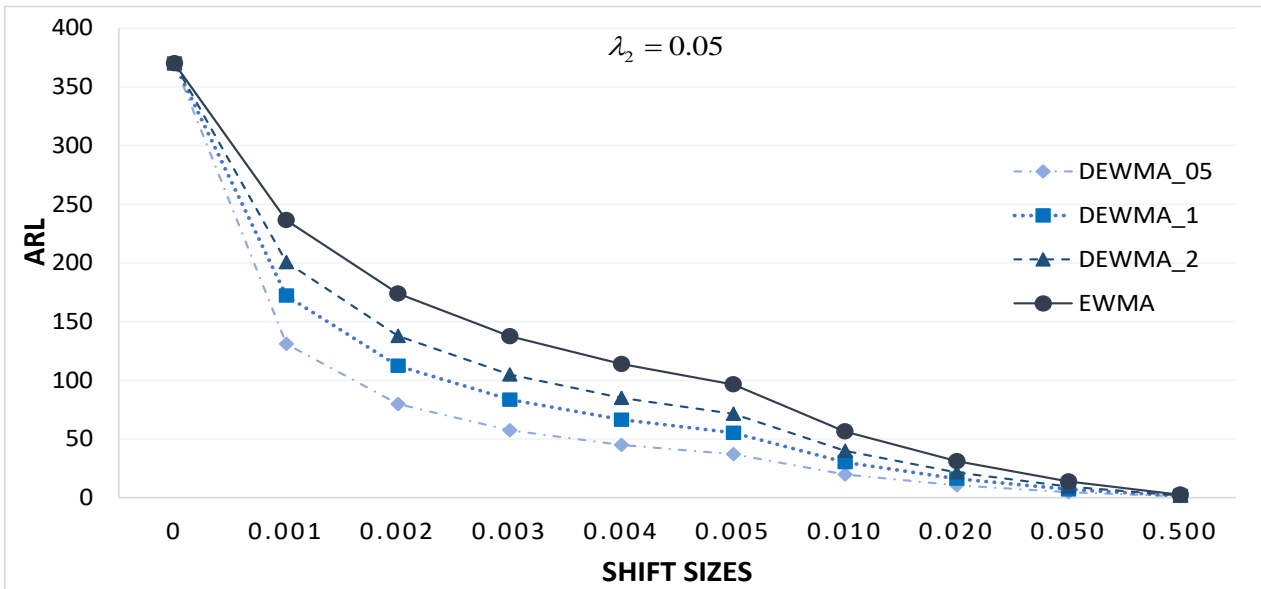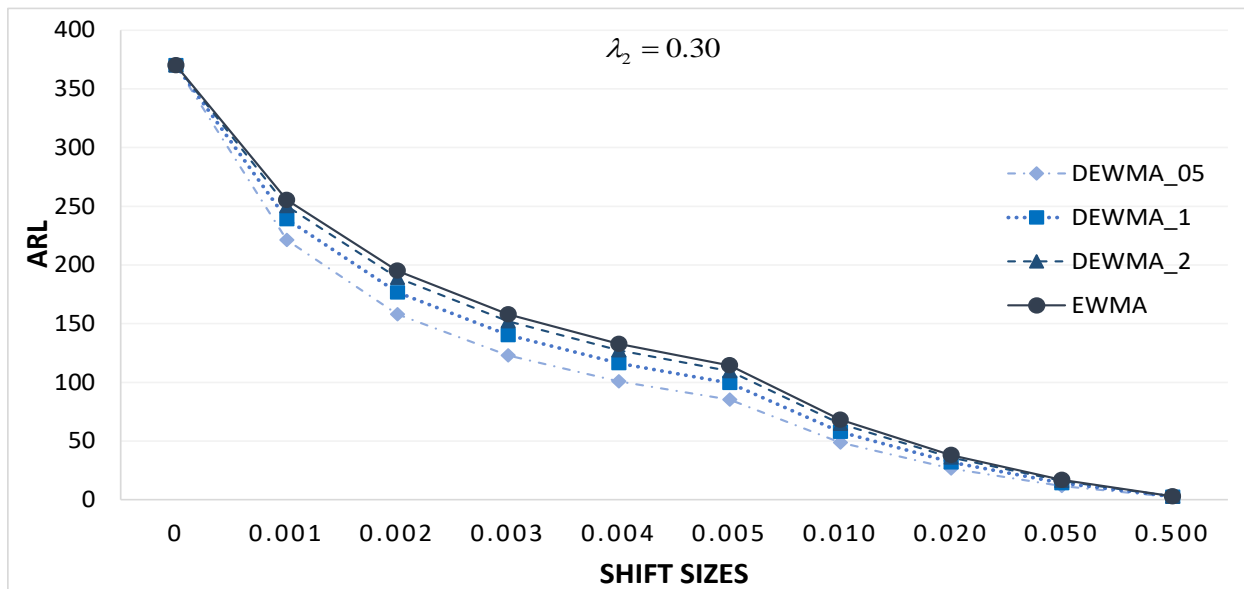
Fig. 1. Comparison of the ARL values based on the DEWMA with different λ_2 and the EWMA control charts on the SAR(1)$_{12}$ model.
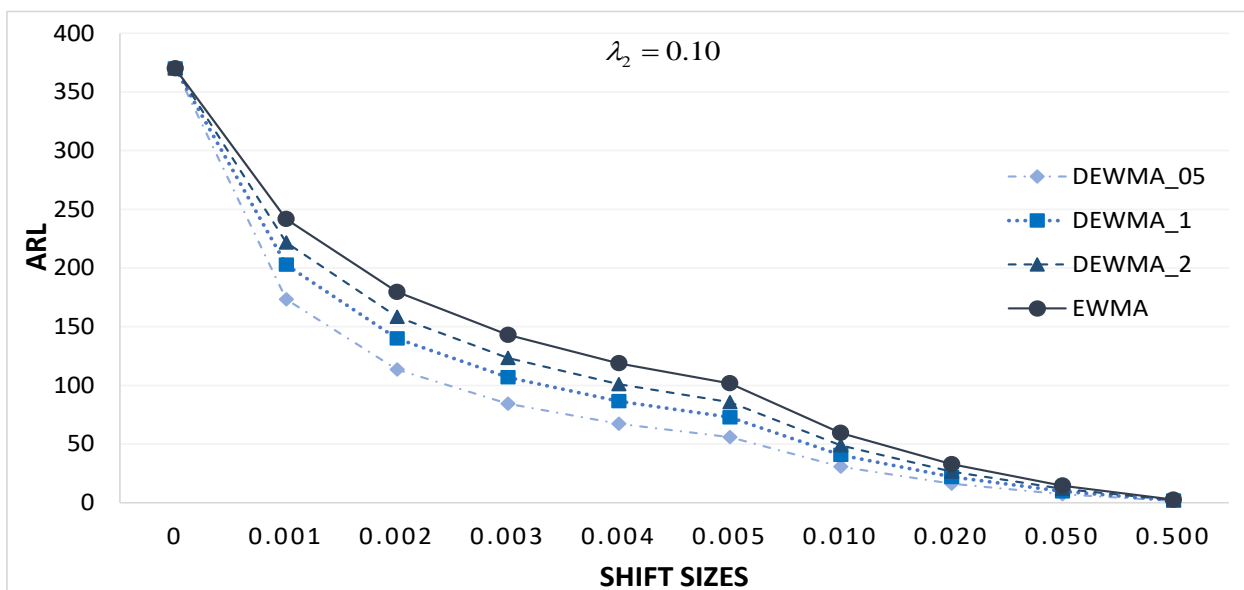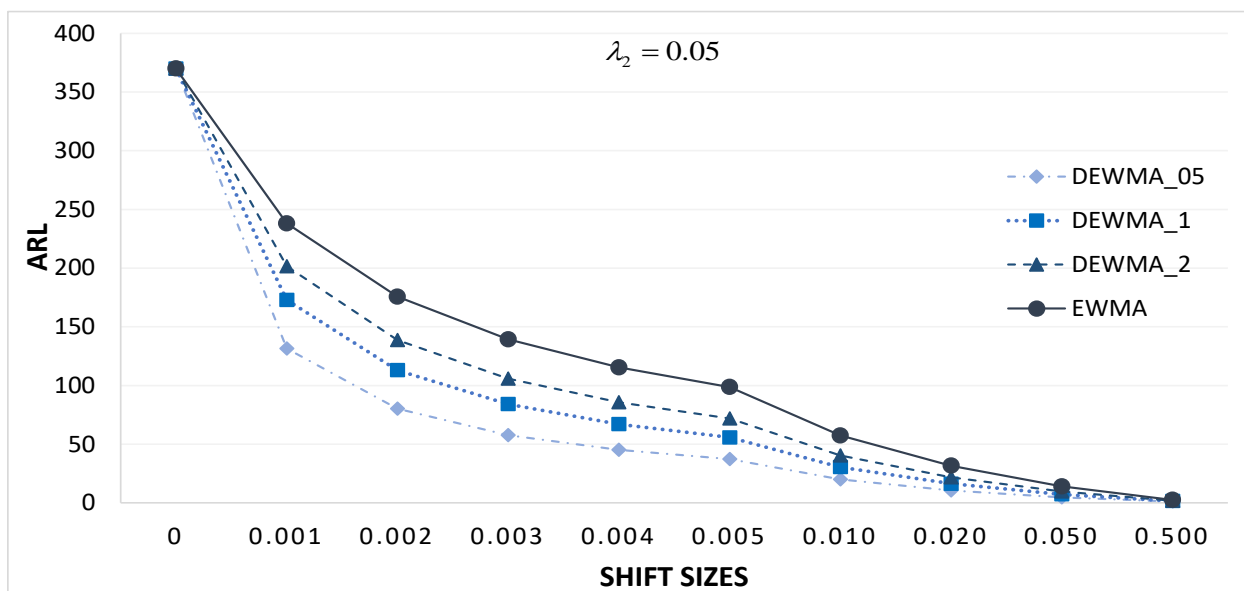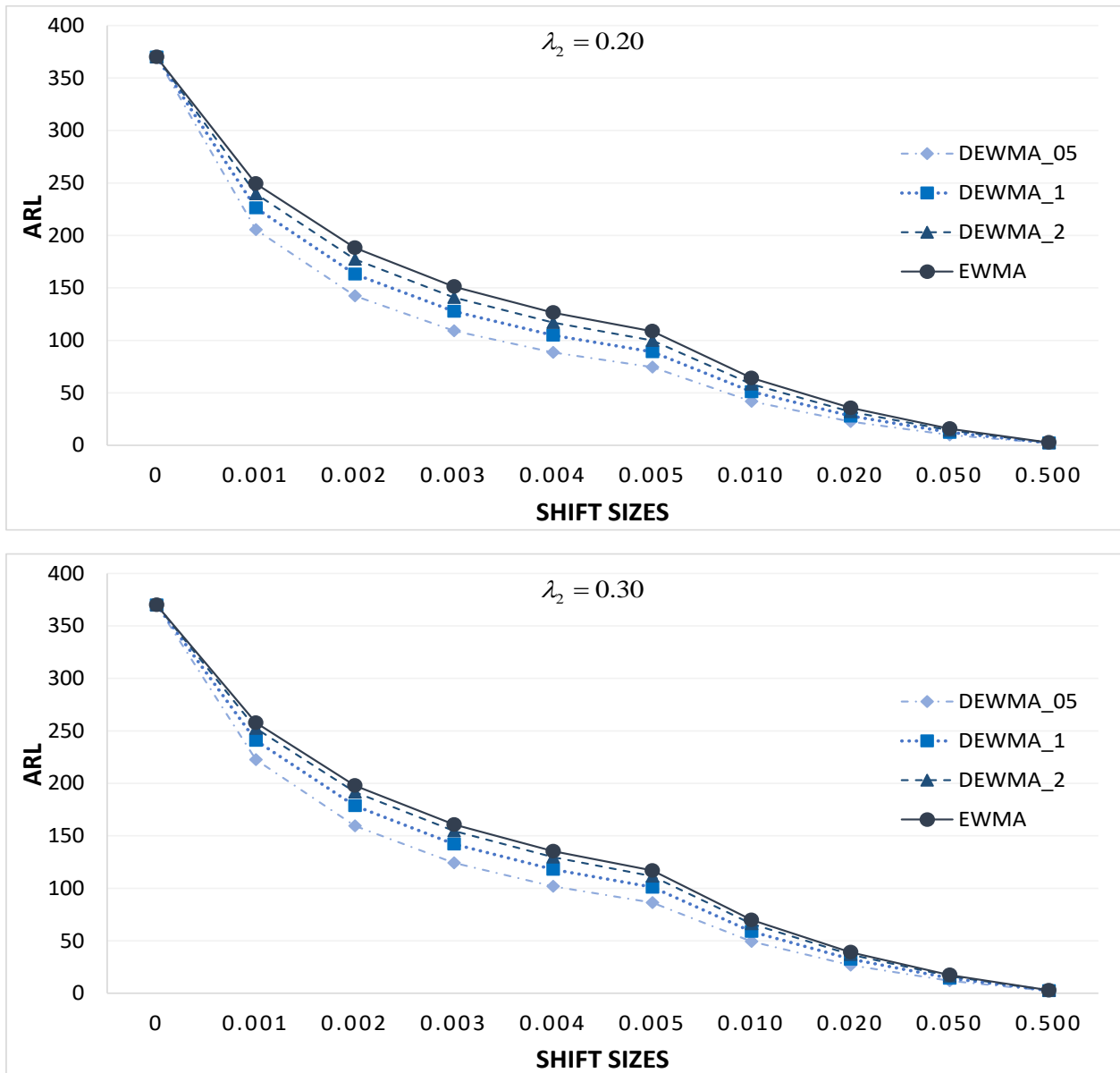
Fig. 2. Comparison of the ARL values based on the DEWMA with different λ_2 and the EWMA control charts on the SAR(2)$_{12}$ model.

IV. APPLICATION OF THE PROPOSED EXPLICIT ARL

Air pollution is one of Thailand's most important environmental problems. For people who reside in and travel to tourist cities where air pollution levels are substantially higher, the effects of the issue are particularly severe. As a result, air pollution is a major issue in Thailand that requires quick attention. This study looked at two types of air pollutant concentrations: particulate matter (PM10) in terms of micrograms per cubic meter ($\mu g / m^3$) and ozone (O₃) in terms of ppb in Chiang Mai, Thailand, with statistical process control used to monitor and detect when the concentrations of air pollutants exceeded the specified limits. Monthly observations of seasonally fitted models served as evidence that the data were real. There are two case studies of models that are running on the DEWMA and compared to the EWMA control chart.

Both real data consist of 48 observations of the monthly concentrations of PM10 and O₃ from January 2017 to December 2020, which were downloaded from a website: http://inenvocc.ddc.moph.go.th/dust/ and shown in Fig. 3. Furthermore, the SAR model was fitted using the SPSS program, and the Kolmogorov-Smirnov test was used to defined that exponential distribution using residuals. The coefficient values for the SAR(p)ₛ model that was used in this case study are shown in Table VI and VII.

TABLE V
RMI AND AEQL VALUES FOR IN THE INDICATED CAPABILITY OF CHARTS.

Control Charts			λ_2 0.05	0.1	0.2	0.3
			SAR(1)₁₂ model			
DEWMA	$\lambda_1 = 0.5\lambda_2$	RMI	**0.0000**	**0.0000**	**0.0000**	**0.0000**
		AEQL	**0.0325**	**0.0411**	**0.0514**	**0.0582**
	$\lambda_1 = \lambda_2$	RMI	0.3984	0.2493	0.1649	0.1413
		AEQL	0.0410	0.0507	0.0605	0.0674
	$\lambda_1 = 2\lambda_2$	RMI	0.7518	0.4412	0.2861	0.2429
		AEQL	0.0504	0.0590	0.0675	0.0740
EWMA	$\lambda_1 = 1$	RMI	1.3318	0.6792	0.3834	0.2936
		AEQL	0.0680	0.0695	0.0731	0.0774
			SAR(2)₁₂ model			
DEWMA	$\lambda_1 = 0.5\lambda_2$	RMI	**0.0000**	**0.0000**	**0.0000**	**0.0000**
		AEQL	**0.0326**	**0.0413**	**0.0518**	**0.0589**
	$\lambda_1 = \lambda_2$	RMI	0.4008	0.2514	0.1678	0.1451
		AEQL	0.0412	0.0511	0.0613	0.0684
	$\lambda_1 = 2\lambda_2$	RMI	0.7574	0.4465	0.2927	0.2512
		AEQL	0.0508	0.0596	0.0685	0.0755
EWMA	$\lambda_1 = 1$	RMI	1.3544	0.6923	0.3944	0.3045
		AEQL	0.0689	0.0705	0.0744	0.0790

Note: The results are bold because they have the lowest of RMI and AEQL values.

TABLE VI
THE SAR(1)₁₂ MODEL COEFFICIENT VALUES WERE CALCULATED USING PM10 CONCENTRATIONS IN THAILAND AS CASE STUDY 1.

Variable	Coefficient	SE	t	Sig
c	48.377	7.436	6.506	0.000
AR(1)	0.894	0.064	13.868	0.000
One-Sample Kolmogorov-Smirnov test				
Exponential parameter			14.0799	
Kolmogorov-Smirnov			0.534	
Asymp.Sig (2-tailed)			0.938	

TABLE VII
THE SAR(3)₁₂ MODEL COEFFICIENT VALUES WERE CALCULATED USING O₃ CONCENTRATIONS IN THAILAND AS CASE STUDY 2.

Variable	Coefficient	SE	t	Sig
c	27.385	2.949	9.287	0.000
AR(1)	0.597	0.159	3.744	0.001
AR(2)	-0.472	0.173	-2.724	0.009
AR(3)	0.835	0.084	9.877	0.000
One-Sample Kolmogorov-Smirnov test				
Exponential parameter			6.6258	
Kolmogorov-Smirnov			1.246	
Asymp.Sig (2-tailed)			0.090	

The concentrations of PM10 in Thailand was determined as SAR(1)₁₂ model and the parameters were shown in Table VI. So, the SAR(1)₁₂ model is expressed as follows:

$$X_t = 48.377 + 0.894 X_{t-12} + \varepsilon_t; \varepsilon_t \sim Exp(14.0799).$$
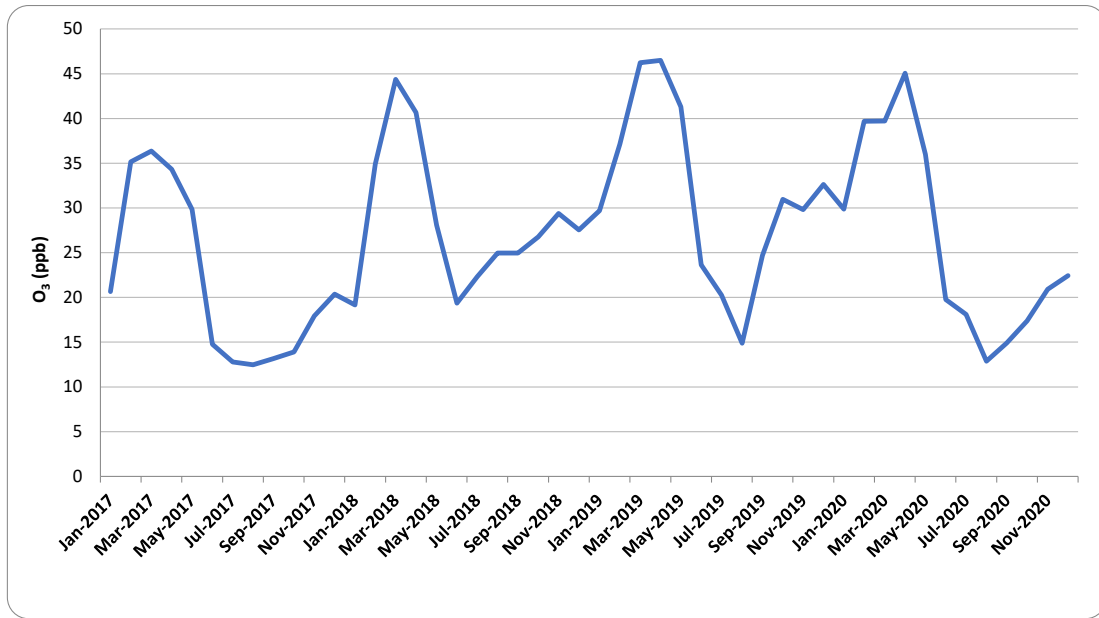
The concentrations of O₃ in Thailand was determined as SAR(3)₁₂ model and the parameters were shown in Table VII. So, the SAR(3)₁₂ model is expressed as follows:

$$X_t = 27.385 + 0.597 X_{t-12} - 0.472 X_{t-24} + 0.835 X_{t-36} + \varepsilon_t;$$

$\varepsilon_t \sim Exp(6.6258)$. The results of fitting the SAR(1)₁₂ model from Table VIII to the dataset containing PM10 concentrations show that the DEWMA control chart with the exponential smoothing parameter relative to $\lambda_1 = 0.5\lambda_2$ has the lowest ARL based on shift changes when compared to the DEWMA with another exponential smoothing parameter and the EWMA control charts. Thus, the DEWMA with a lower exponential smoothing parameter is more efficient than the DEWMA with a higher exponential smoothing parameter, and it also outperforms the EWMA control chart in all situations. According to the results of applying the SAR(3)₁₂ model from Table IX. to the dataset containing O₃ concentrations, the DEWMA control chart with the exponential smoothing parameter relative to $\lambda_1 = 0.5\lambda_2$ has the lowest ARL based on shift changes, which is in conformity with the SAR(1)₁₂ model's findings. The ARL values are based on various shift sizes shown in graphs in Fig. 4. and 5.

Furthermore, the lowest RMI and AEQL values in Table X, particularly for DEWMA, which result from the lower exponential smoothing parameter values, are consistent with the efficacy of the DEWMA control chart. As a result, the results indicated that the PM10 and O₃ concentration datasets in Thailand studied gave the same results as the simulated data.

Additionally, the effectiveness of the shift change detection procedure shows that, under identical circumstances, the DEWMA control chart identifies shift changes better than the EWMA control chart. Notice the graphs in Figs. 6 and 7. The detection on the DEWMA control chart Based on observations made using the SAR(1)₁₂ model, it exceeded the bound for the first time at the first observation, which can be detected more quickly than the EWMA control chart, which did so at the 15th observation. Similarly, the DEWMA control chart recognized that it had exceeded the bound for the first time at the 6th observation when it came to identifying shift changes in observations conducted on the SAR(3)₁₂ model, whereas the EWMA control chart surpassed the bound after the 15th observation.

(A)
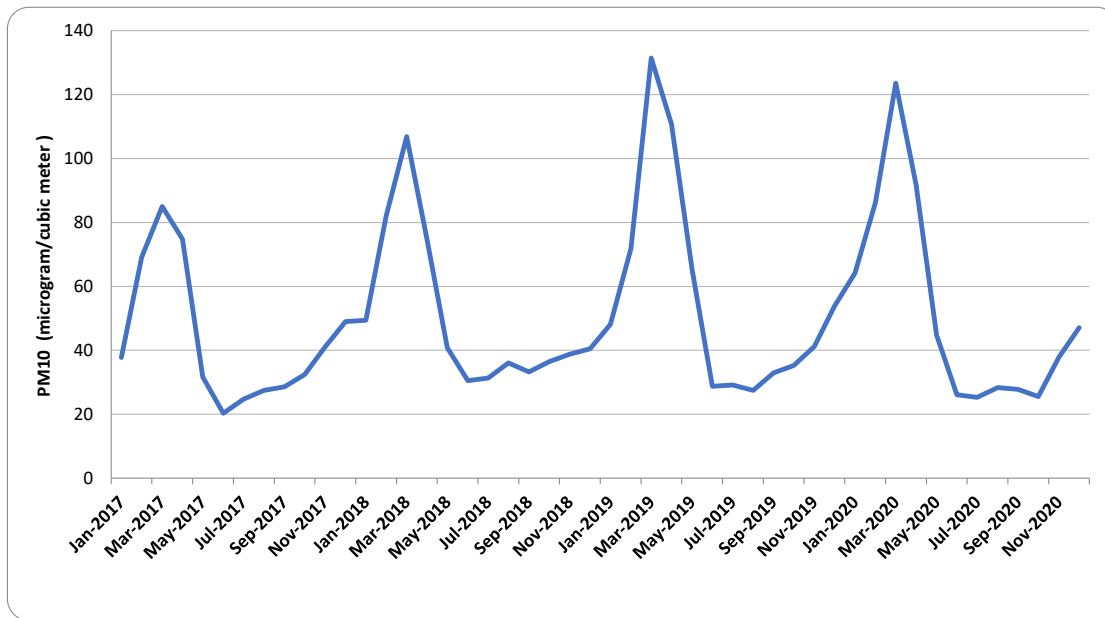
(B)

Fig.3. The real data of the concentrations of air pollutants in Thailand, namely: (A) PM10 ($\mu g / m^3$) and (B) O$_3$ (ppb).

TABLE VIII

PERFORMANCE COMPARISON ON THE DEWMA WITH $\lambda_1 = 0.5\lambda_2$ AND EWMA CONTROL CHARTS, AND DIFFERENT SHIFT SIZES IN THE MODEL WERE PERFORMED WITH SAR(1)$_{12}$ BY USING THE DATASET OF PM10 CONCENTRATIONS IN THAILAND, AND DETERMINED c AND ϕ_1 EQUAL TO 48.377 AND 0.894, RESPECTIVELY.

λ_2	Control Charts	λ_1	b	Shift sizes (δ)									
				0	0.001	0.002	0.003	0.004	0.005	0.01	0.02	0.05	0.5
0.05	DEWMA	$\lambda_1 = 0.5\lambda_2$	0.0000668327	370	108.13	63.53	45.19	35.07	28.70	15.23	8.09	3.68	1.12
		$\lambda_1 = \lambda_2$	0.00055342	370	127.14	76.97	55.41	43.28	35.56	18.98	10.07	4.51	1.20
		$\lambda_1 = 2\lambda_2$	0.00225279	370	139.12	85.86	62.32	48.91	40.29	21.62	11.47	5.10	1.27
	EWMA	$\lambda_1 = 1$	0.04272205	370	151.62	95.55	69.99	55.21	45.63	24.64	13.09	5.80	1.35
0.1	DEWMA	$\lambda_1 = 0.5\lambda_2$	0.001107274	370	127.17	76.99	55.43	43.30	35.57	18.99	10.07	4.51	1.20
		$\lambda_1 = \lambda_2$	0.00450918	370	139.20	85.92	62.37	48.95	40.32	21.64	11.48	5.11	1.27
		$\lambda_1 = 2\lambda_2$	0.0128723	370	145.95	91.11	66.46	52.30	43.16	23.24	12.34	5.47	1.31
	EWMA	$\lambda_1 = 1$	0.0855738	370	151.79	95.68	70.10	55.29	45.70	24.68	13.12	5.80	1.35
0.2	DEWMA	$\lambda_1 = 0.5\lambda_2$	0.0090328	370	139.35	86.04	62.47	49.02	40.39	21.68	11.50	5.12	1.27
		$\lambda_1 = \lambda_2$	0.02580356	370	146.20	91.30	66.61	52.42	43.26	23.30	12.37	5.48	1.31
		$\lambda_1 = 2\lambda_2$	0.06168995	370	149.86	94.15	68.88	54.29	44.84	24.19	12.85	5.69	1.33
	EWMA	$\lambda_1 = 1$	0.1716695	370	152.12	95.94	70.31	55.47	45.85	24.76	13.16	5.82	1.35

TABLE IX

PERFORMANCE COMPARISON ON THE DEWMA WITH $\lambda_1 = 0.5\lambda_2$ AND EWMA CONTROL CHARTS, AND DIFFERENT SHIFT SIZES IN THE MODEL WERE PERFORMED WITH SAR(3)$_{12}$ BY USING THE DATASET OF O$_3$ CONCENTRATIONS IN THAILAND, AND DETERMINED c, ϕ_i ; $i = 1, 2, 3$ EQUAL TO 27.385, 0.597, -0.472, AND 0.835, RESPECTIVELY.

λ_2	Control Charts	λ_1	b	Shift sizes (δ)									
				0	0.001	0.002	0.003	0.004	0.005	0.01	0.02	0.05	0.5
0.05	DEWMA	$\lambda_1 = 0.5\lambda_2$	0.0000746943	370	119.44	70.99	50.83	39.66	32.55	17.31	9.19	4.14	1.16
		$\lambda_1 = \lambda_2$	0.000676301	370	144.14	89.19	64.95	51.14	42.22	22.67	12.05	5.35	1.29
		$\lambda_1 = 2\lambda_2$	0.00288022	370	160.01	101.69	74.94	59.40	49.24	26.67	14.20	6.27	1.41
	EWMA	$\lambda_1 = 1$	0.0569306	370	176.55	115.53	86.30	68.94	57.44	31.45	16.82	7.41	1.56
0.1	DEWMA	$\lambda_1 = 0.5\lambda_2$	0.001353981	370	144.24	89.27	65.02	51.19	42.26	22.70	12.06	5.35	1.29
		$\lambda_1 = \lambda_2$	0.00577297	370	160.19	101.87	75.08	59.52	49.35	26.73	14.24	6.29	1.41
		$\lambda_1 = 2\lambda_2$	0.01687272	370	169.23	109.32	81.17	64.61	53.71	29.26	15.62	6.88	1.48
	EWMA	$\lambda_1 = 1$	0.1143535	370	177.07	115.97	86.66	69.25	57.71	31.60	16.90	7.44	1.56
0.2	DEWMA	$\lambda_1 = 0.5\lambda_2$	0.01159655	370	160.68	102.26	75.41	59.79	49.57	26.86	14.31	6.31	1.41
		$\lambda_1 = \lambda_2$	0.03396255	370	170.00	109.96	81.68	65.04	54.08	29.47	15.73	6.93	1.49
		$\lambda_1 = 2\lambda_2$	0.0822512	370	174.97	114.17	85.17	67.98	56.61	30.96	16.54	7.28	1.53
	EWMA	$\lambda_1 = 1$	0.2307105	370	178.08	116.85	87.39	69.87	58.24	31.92	17.07	7.51	1.56

TABLE X

RMI AND AEQL VALUES WERE USED IN THE INDICATED CAPABILITY OF CONTROL CHARTS WHEN THE PARAMETERS OF SAR(1)$_{12}$ AND SAR(3)$_{12}$ WERE OBTAINED BY TWO DATASETS OF PM10 AND O$_3$ CONCENTRATIONS IN THAILAND, RESPECTIVELY.

Control Charts			SAR(1)$_{12}$ model			SAR(3)$_{12}$ model		
			$\lambda_2 = 0.05$	$\lambda_2 = 0.1$	$\lambda_2 = 0.2$	$\lambda_2 = 0.05$	$\lambda_2 = 0.1$	$\lambda_2 = 0.2$
DEWMA	$\lambda_1 = 0.5\lambda_2$	RMI	**0.0000**	**0.0000**	**0.0000**	**0.0000**	**0.0000**	**0.0000**
		AEQL	**0.0295**	**0.0320**	**0.0339**	**0.0308**	**0.0347**	**0.0380**
	$\lambda_1 = \lambda_2$	RMI	0.1879	0.1066	0.0567	0.2355	0.1358	0.0745
		AEQL	0.0319	0.0339	0.0351	0.0347	0.0379	0.0402
	$\lambda_1 = 2\lambda_2$	RMI	0.3175	0.1703	0.0879	0.4071	0.2197	0.1164
		AEQL	0.0339	0.0351	0.0358	0.0379	0.0401	0.0415
EWMA	$\lambda_1 = 1$	RMI	0.4639	0.2275	0.1077	0.6084	0.2967	0.1434
		AEQL	0.0362	0.0362	0.0363	0.0421	0.0422	0.0424

Note: The results are bold because they have the lowest of RMI and AEQL values.
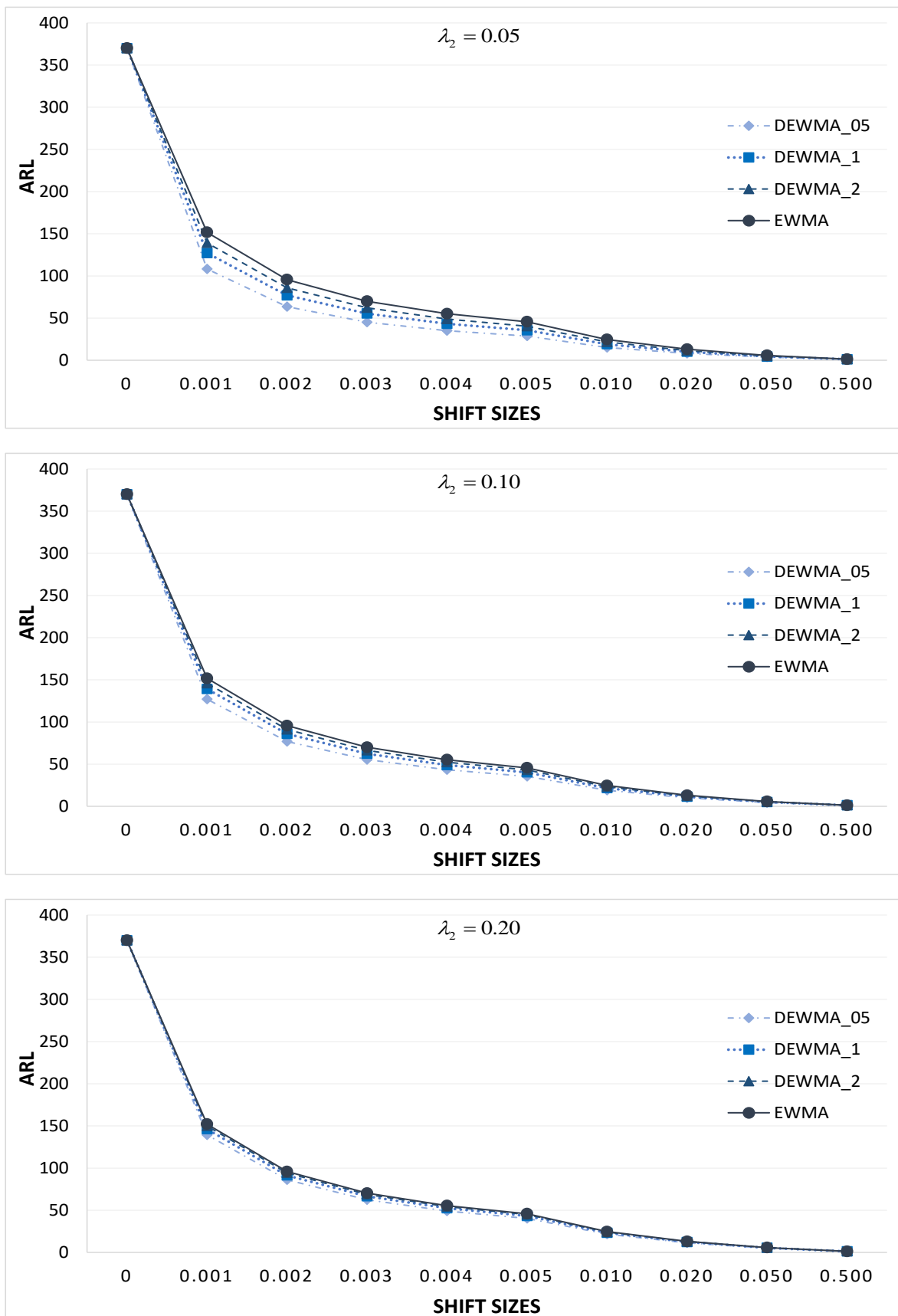
Fig. 4. Comparison of the ARL values based on the DEWMA with different λ_2 and the EWMA charts based on the SAR(1)$_{12}$ model by using the dataset of PM10 concentrations in Thailand
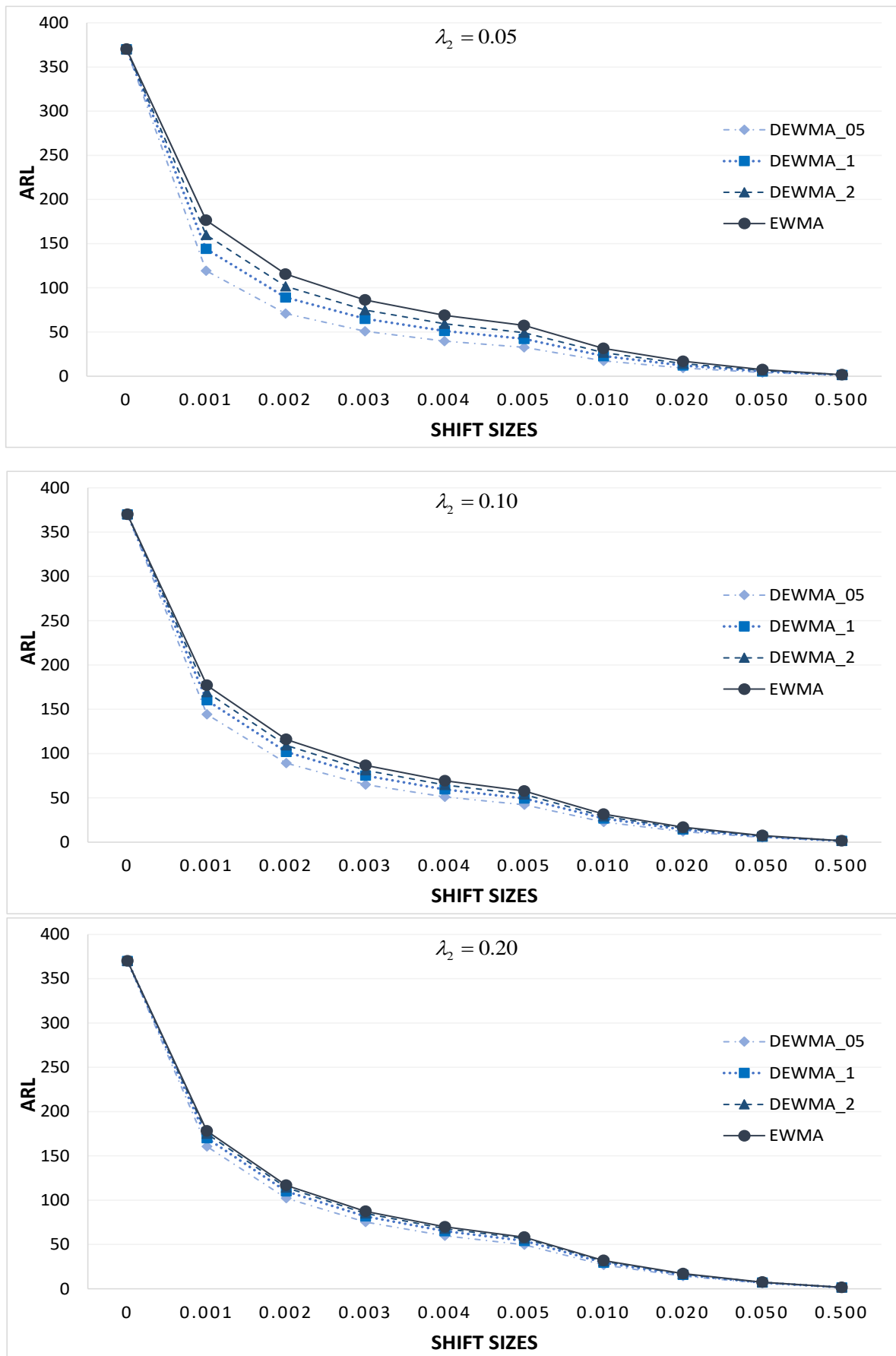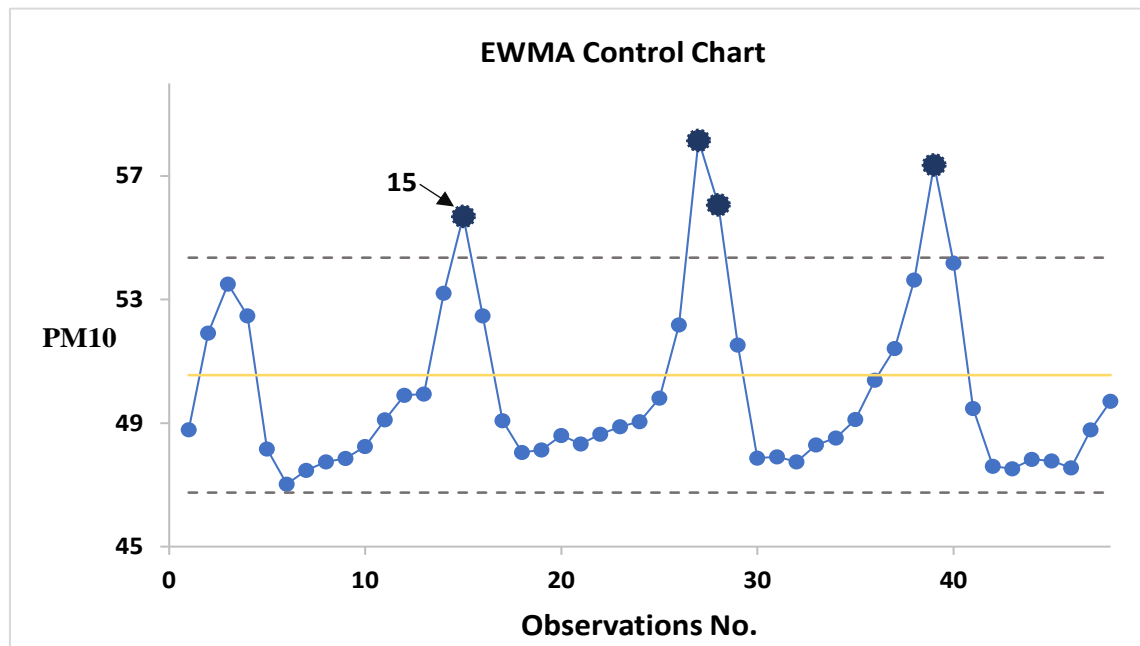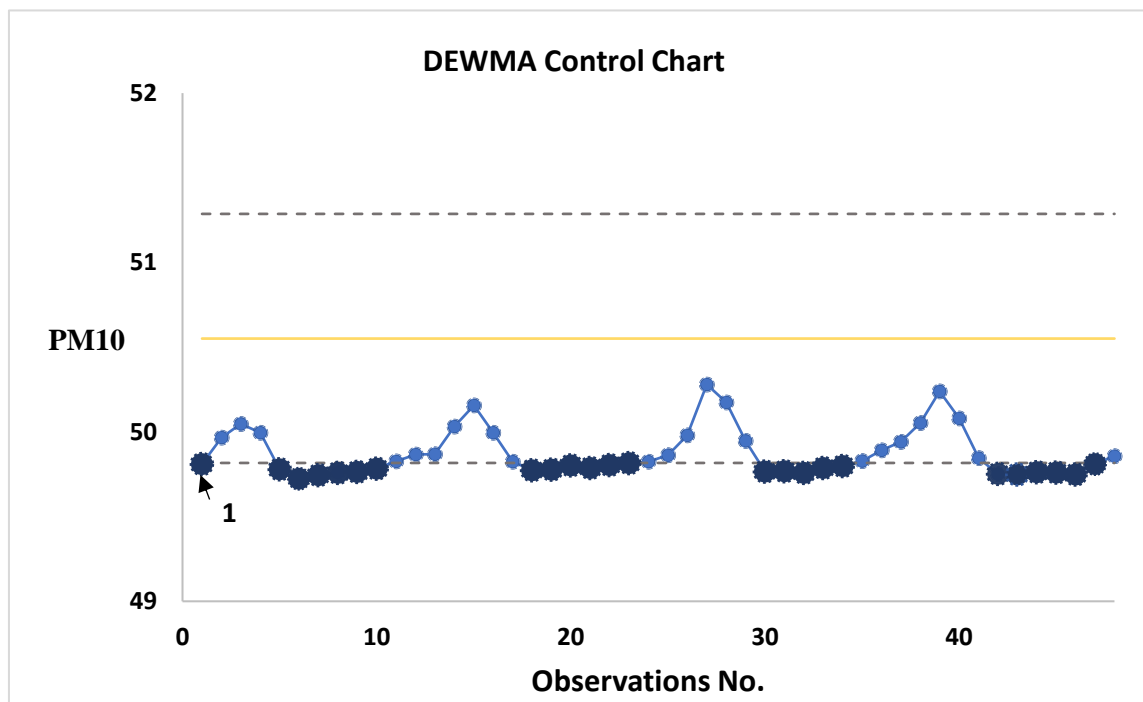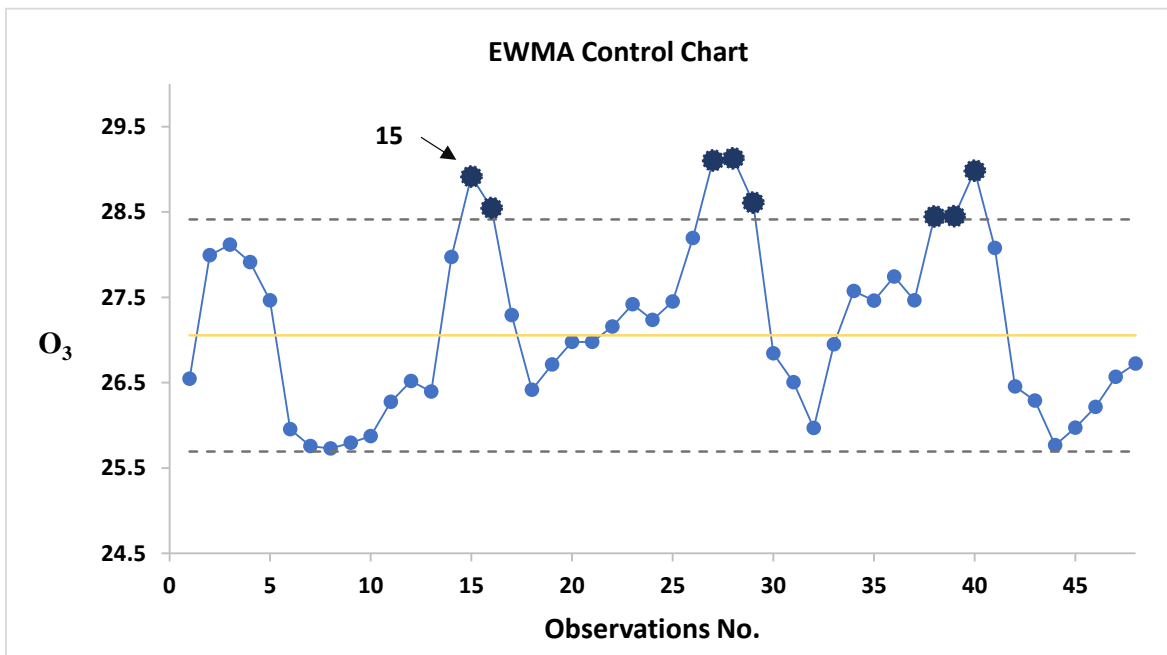
Fig. 5. Comparison of the ARL values based on the DEWMA with different λ_2 and the EWMA charts based on the SAR(3)$_{12}$ model by using the dataset of O$_3$ concentrations in Thailand
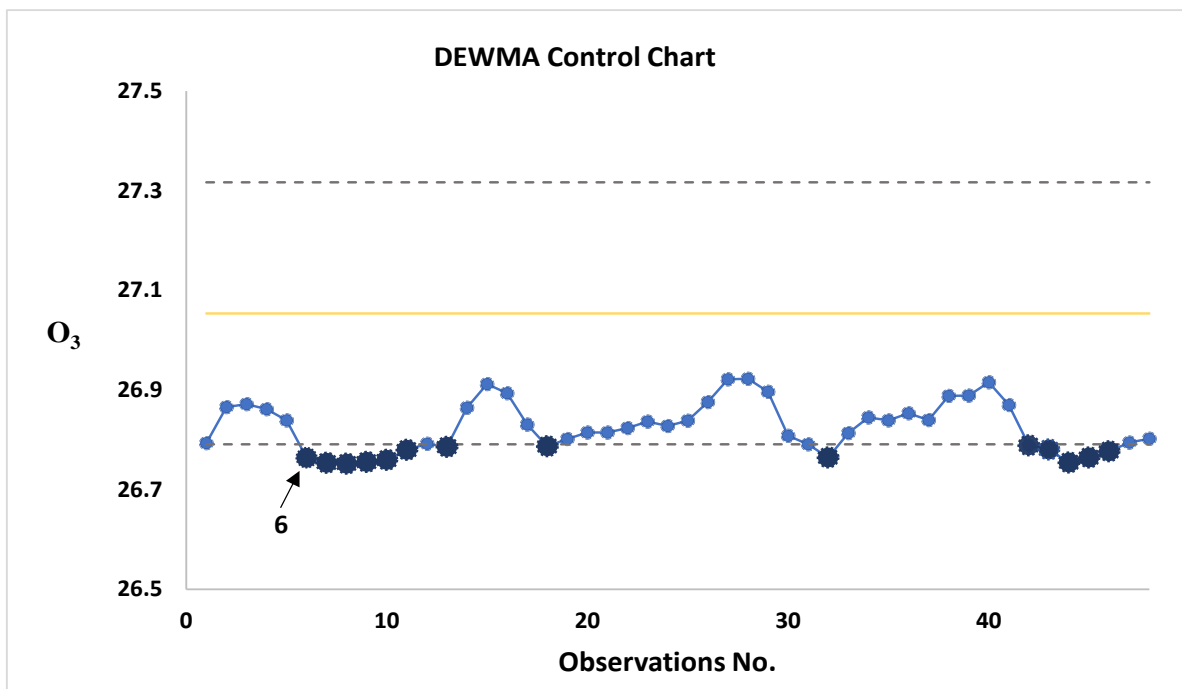
(A)

(B)

Fig. 6. The capability of detecting processes in the dataset, which is PM10 concentrations based on the $SAR(1)_{12}$ model and running on two control charts; (A) EWMA and (B) DEWMA control charts.

(A)

(B)

Fig. 7. The capability of detecting processes in the dataset, which is O_3 concentrations based on the $SAR(3)_{12}$ model and running on two control charts; (A) EWMA and (B) DEWMA control charts.

V. CONCLUSIONS

The efficiency of the DEWMA control chart, which runs SAR(p)$_s$ models with an exponential white noise distribution, was evaluated using the explicit ARL, which outperformed the NIE approach's explicit ARL in terms of computation time. After that, the explicit ARL on running the DEWMA control chart was compared to the EWMA control chart in cases of different exponential smoothing parameters for the simulated data, which form the SAR(p)$_s$ model. Two measurements, such as RMI and AEQL, confirm the effectiveness of control charts, and the explicit ARL values were compared for all instances. According to the results, the DEWMA, which has a lower exponential smoothing parameter than the DEWMA, which has a higher exponential smoothing value, may express more capability. The DEWMA control chart also appears to be better than the EWMA control chart in all circumstances. In addition, the explicit ARL can also be applied to real data, which gives the same results as simulated data. In this study, it was applied to the data about the concentration of air pollutants such as PM10 and O$_3$ in Thailand. Hence, the explicit formula is an alternative for calculating the ARL for shift changes, and the case study showed the data with the SAR(p)s model running on the DEWMA control chart.

REFERENCES

[1] Y. Supharakonsakun, Y. Areepong, S. Sukparungsee. The performance of a modified EWMA control chart for monitoring autocorrelated PM2.5 and carbon monoxide air pollution data, PeerJ, 21 pages, 2020.

[2] M. Arslan, S.M. Anwar, S.A. Lone, Z. Rasheed, M. Khan, S.A. Abbasi. Improve adaptive EWMA control chart for process location with applications in groundwater physicochemical parameters and glass manufacturing industry, PLOS ONE, 24 pages, 2022.

[3] W.H. Woodall. The Use of Control Charts in Health-Care and Public-Health Surveillance, Journal of Quality Technology, Vol. 38, No. 2, 89-104, 2006.

[4] W.A. Shewhart. Quality control charts, Bell System Technical Journal, Vol. 5, No. 4, 593-603, 1926.

[5] E.S. Page. Continuous inspection schemes, Biometrika, Vol. 41, No. 1-2, 100-115, 1954.

[6] W.S. Roberts. Control chart tests based on geometric moving averages, Technometrics, Vol. 1, No. 3, 239-250, 1959.

[7] A.K. Patel, J. Divecha. Modified exponentially weighted moving average (EWMA) control chart for an analytical process data, Journal of Chemical Engineering and Materials Science, Vol. 2, 12-20, 2011.

[8] N. Khan, M. Aslam, C.H. Jun. Design of a control chart using a modified EWMA statistic, Quality and Reliability Engineering International, Vol. 33, No. 5, 1095-1104, 2017.

[9] M. Naveed, M. Azam, N. Khan, M. Aslam. Design of a control chart using extended EWMA statistic, Technologies, Vol. 4, No. 6, 108-122, 2018.

[10] K. Karoon, Y. Areepong, S. Sukparungsee. Trend autoregressive model exact run length evaluation on a two-sided extended EWMA chart, Computer Systems Science and Engineering, Vol. 44, No. 2, 1143-1160, 2023.

[11] A.A. Mahmoud, W.H. Woodall. An evaluation of the double exponentially weighted moving average control chart, Communications in Statistics-Simulation and Computation, Vol. 39, No. 5, 933-949, 2010.

[12] S.E. Shamma, A.K. Shamma. Development and evaluation of control charts using double exponentially weighted moving averages, International Journal of Quality Reliability Management, Vol. 9, No. 6, 18-25, 1992.

[13] M.T. Ismail, R.S. Al-Gounmeein. Overview of long memory for economic and financial time series dataset and related time series models: A Review Study, IAENG International Journal of Applied Mathematics, Vol. 52, No. 2, 261-269, 2022.

[14] G.C. Runger, S.S. Prabhu. A Markov Chain Model for the Multivariate Exponentially Weighted Moving Averages Control Chart, Journal of the American Statistical Association, Vol. 91, No. 436, 1701-1706, 1996.

[15] M. Riaz, B. Zaman, I.A. Raji, M.H. Omar, R. Mehmood, N. Abbas. An Adaptive EWMA Control Chart based on Principle Component Method to monitor Process Mean Vector, Mathematics, Vol. 10, 27 pages, 2022.

[16] K. Karoon, Y. Areepong, S. Sukparungsee. Numerical integral equation methods of average run length on extended EWMA control chart for autoregressive process. In proceesing of International Conference on Applied and Engineering Mathematics, London, England, 51-56, 2021.

[17] W. Suriyakat, K. Petcharat. Exact run length computation on EWMA control chart for Stationary moving average process with exogenous variables, Mathematics and Statistics, Vol. 10, No. 3, 624-635, 2022.

[18] K. Petcharat, S. Sukparungsee, Y. Areepong. Exact solution of the average run length for the cumulative sum chart for a moving average process of order q, ScienceAsia, Vol. 41, No. 2, 141-147, 2015.

[19] R. Sunthornwat, Y. Areepong, S. Sukparungsee. Average run length of the long-memory autoregressive fractionally integrated moving average process of the exponential weighted moving average control chart, Cogent Mathematics, Vol. 4, No. 1, 1358536, 2017.

[20] P. Phanthuna, Y. Areepong, Sukparungsee. Detection capability of the modified EWMA chart for trend stationary AR(1) model, Thailand Statistician, Vol. 19, No. 1, 70-81, 2021.

[21] K. Karoon, Y. Areepong, S. Sukparungsee. Exact solution of average run length on extended EWMA control chart for the first-order autoregressive process, Thailand Statistician, Vol. 20, No. 2, 395-411, 2022.

[22] K. Karoon, Y. Areepong, S. Sukparungsee. Exact run length evaluation on Extended EWMA control chart for autoregressive process, Intelligent Automation and Soft Computing, Vol. 33, No. 2, 743-759, 2022.

[23] K. Karoon, Y. Areepong, S. Sukparungsee. On the performance of the extended EWMA control chart for monitoring process mean based on autocorrelated data, Applied Science and Engineering Process, Vol. 16, No. 4, 6599, 2023.

[24] K. Silpakob, Y. Areepong, S. Sukparungsee, R. Sunthornwat. Exact average run length evaluation for an ARMAX(p,q,r) process running on a modified EWMA control chart, IAENG International Journal of Applied Mathematics, Vol. 53, No. 1, 266-276, 2023.

[25] K. Karoon, Y. Areepong, S. Sukparungsee. Modification of ARL for detecting changes on the double EWMA chart in time series data with the autoregressive model, Connection Science, Vol. 35, No. 1, 2219040, 2023.

[26] P. Phanthuna, Y. Areepong. Analytical solution of ARL for SAR(p)$_L$ model on a modified EWMA chart, Mathematics and Statistics, Vol. 9, No. 5, 685-696, 2021.

[27] S. Phanyaem. Explicit formulas and numerical integral equation of ARL for SARX(P,r)$_L$ model based on CUSUM chart, Mathematics and Statistics, Vol. 10, No. 1, 88-99, 2022.

[28] K. Petcharat. The effectiveness of CUSUM control chart for trend stationary seasonal autocorrelated Data, Thailand Statistician, Vol. 20, No. 2, 475-488.

[29] K. Karoon, Y. Areepong, S. Sukparungsee. Exact run length evalution on extended EWMA control chart for seasonal

autoregressive process, Engineering Letters, Vol. 30, No. 2, 1377-1390, 2022.

[30] C. Chananet, S. Phanyaem. Improving CUSUM control chart for monitoring a change in processes based on seasonal ARX model, IAENG International Journal of Applied Mathematics, Vol. 52, No. 3, 589-596, 2022.

[31] K. Petcharat. Designing the Performance of EWMA control chart for seasonal moving average process with exogenous variable, IAENG International Journal of Applied Mathematics, Vol. 53, No. 2, 757-765, 2023.

[32] K. Chen, C.A. Wang. A hybrid SARIMA and support vector Machines in forecasting the production values of the machinery industry in Taiwan, Expert System with Applications, Vol. 32, 254-264, 2007.

[33] E. Montaser, J.L. Diez, J. Bondia. Stochastic seasonal models for glucose prediction in the artificial pancreas, Journal of Diabetes Science and Technology, Vol. 11, No. 6, 1124-1131, 2017.

[34] F. Kadri, F. Harrou, S. Chaabane, Y. Sun, C. Tahon. Seasonal ARMA-based SPC chart for anomaly detection: Application to emergency depertment systems, Neurocomputing, Elsevier, Vol. 173, No. 3, 2102-2114, 2016.

[35] M. Almousa. Adomian decomposition method with modified Bernstein polynomials for solving nonlinear Fredholm and Volterra integral equations, Mathematics and Statistics, Vol. 18, No. 3, 278-285, 2020.

[36] S. Shukla, S. Balasubramanian, M.A. Pavlovic. Generalized Banach fixed point theorem, Bulletin of the Malaysian Mathematical Sciences Society, Vol. 39, 1529-1539, 2016.

[37] A. Tang, P. Castagliola, J. Sun, and X. Hu. Optimal design of the adaptive EWMA chart for the mean based on median run length and expected median run length, Quality Technology and Quantitative Management, Vol. 16, No. 4, 439-458, 2018.

[38] V. Alevizakos, K. Chatterjee, C. Koukouvinos. The triple exponentially weighted moving average control chart, Quality Technology & Quantitative Management, Vol. 18, No. 3, 326-354, 2021.